ARAB ACADEMY FOR SCIENCE, TECHNOLOGY AND MARITIME TRANSPORT

College of Engineering and Technology

Mechanical Engineering Department

Enhancing Efficiency of Darrieus Wind Turbines through Experimental and Numerical Investigations of Double Darrieus Configurations

By

Israa Idris Abdelkarim Idris

A thesis submitted to AASTMT in partial

Fulfillment of the requirements for the award of the degree of

MASTER OF SCIENCE

in

MECHANICAL ENGINEERING

Supervisors

Prof. Yehia A. Eldrainy
Mechanical Engineering Department
Faculty of Engineering
Alexandria University
Alexandria

Dr. Rola S. Afify
Mechanical Engineering Department
College of Engineering and Technology
Arab Academy for Science and Technology and Maritime Transport
Alexandria

Dr. Iham F. Zidane
Mechanical Engineering Department
College of Engineering and Technology
Arab Academy for Science and Technology and Maritime Transport – Alexandria

2023

ARAB ACADEMY FOR SCIENCE, TECHNOLOGY AND MARITIME TRANSPORT

College of Engineering and Technology

Mechanical Engineering Department

Enhancing Efficiency of Darrieus Wind Turbines through Experimental and Numerical Investigations of Double Darrieus Configurations

By

Israa Idris Abdelkarim Idris

A thesis submitted to AASTMT in partial
Fulfillment of the requirements for the award of the degree of

MASTER OF SCIENCE

in

MECHANICAL ENGINEERING

Supervisors

Prof. Yehia A. Eldrainy
Mechanical Engineering Department
Faculty of Engineering,
Alexandria University
Alexandria

Dr. Rola S. Afify
Mechanical Engineering Department
College of Engineering and Technology
Arab Academy for Science and Technology
and Maritime Transport
Alexandria

Dr. Iham F. Zidane
Mechanical Engineering Department
College of Engineering and Technology
Arab Academy for Science and Technology
and Maritime Transport – Alexandria

2023

DECLARATION

I certify that all the material in this thesis that is not my own work has been identified, and that no material is included for which a degree has previously been conferred on me.

The contents of this thesis reflect my own personal views, and are not necessarily endorsed by the University.

Name Israa Idris Abdelkarim Idris .....

Signature .....

Date .....

We certify that we have read the present work and that in our opinion it is fully adequate in scope and quality as a thesis towards the partial fulfillment of the Master's Degree requirements in

Mechanical Engineering

Israa Idris Abdelkarim Idris

From
College of Engineering and Technology
AASTMT

Supervisors:

Name:	**Prof. Dr Yehia A. Eldrainy**
Position:	**Professor of Mechanical Engineering, Faculty of Engineering, Alexandria ،University, Alexandria**
Signature:	
Name:	**Dr. Rola Samir Afify**
Position:	**،Associate Professor of Mechanical Engineering, College of Engineering Arab Academy for Science & Technology & Maritime Transport, Alexandria.**
Signature:	
Name:	**Dr. Iham F. Zidane**
Position:	**Assistant Professor of Mechanical Engineering, College of Engineering, Arab Academy for Science & Technology & Maritime Transport, Alexandria.**
Signature:	

Examiners:

Name:	**Prof. Aly Ismail Shehata**
Position:	**Professor of Mechanical Engineering, College of Engineering, Arab Academy for Science & Technology & Maritime Transport, Alexandria.**
Signature:	
Name:	**Prof. Wael El-Maghlany**
Position:	**Professor of Mechanical Engineering, Faculty of Engineering, Alexandria University, Alexandria**
Signature:	

Name:	**Prof. Dr. Rola Samir Afify**
Position:	**Associate Professor of Mechanical Engineering, College of Engineering, Arab Academy for Science & Technology & Maritime Transport, Alexandria.**
Signature:	

Acknowledgments

I would like to say a big thank you to my thesis advisor, Dr. Rola S. Afify. She has been a great help and support during my research. I really appreciate that she was always available to give me advice when I had questions or problems. Even though she let me work on my own, her guidance always pointed me in the right direction.

I also want to thank Prof. Dr. Yehia A. Eldrainy. His comments and feedback really made my work better, he was always available to give me advice when I had questions or problems, and I'm thankful for his help.

I'd also like to show my appreciation to Dr. Iham F. Zidane for His comments and suggestions while supervising my thesis were very valuable to my research.

I'm thankful to Prof. Dr. Ali Ismaiel, the Head of the Mechanical Engineering Department, and Prof. Dr. Alaa El-Din Khalil, the Vice Dean for Postgraduate Studies and Scientific Research, for their constant support and encouragement throughout my academic journey. They believed in me, and that kept me going.

Lastly, I want to extend my heartfelt thanks to my parents and my family, who have always been my pillars of support throughout my academic journey. Their love and encouragement have been my motivation.

Abstract

This research presents a comprehensive investigation into the performance and aerodynamic characteristics of a double-blade Darrieus wind turbine employing the NACA 0018 airfoil. The study employs a dual approach, combining wind tunnel experimentation with numerical simulations facilitated by Ansys software, to scrutinize the turbine's behavior under varying wind conditions. Experimental measurements encompass torque and power output, while computational fluid dynamics simulations yield insights into flow patterns and pressure distribution. The results conspicuously demonstrate a close concordance between the outcomes of experimental and numerical methodologies, thus affirming the computational model's precision. Additionally, the analysis underscores the profound influence of wind speed on turbine performance, shedding light on the advantageous aerodynamic traits of the NACA 0018 These findings make substantive contributions to the domain of wind turbine design optimization and furnish valuable insights that have implications for forthcoming research in renewable energy. Moreover, this research pinpoints the optimal configuration in the experimental approach for the double-blade Darrieus vertical axis wind turbine. The results revealed that the most efficient position is situated at a distance of 4 cm and 3 cm from the rotor, which corresponded to 40% to 30% in terms of the distance ratio. Notably, a 6.7% Power coefficient improvement is observed when comparing single blade and double blade numerical results.

Table of Contents Page

List of Tables

List of Figures

List of Figures (Cont'd)

Nomenclature

Symbols	Nomenclatures	Unit
A	Area	(m^2)
c	Cord Length	(m)
Cp	Power Coefficient	
Ct	Torque Coefficient	
D	Rotor Diameter	(m)
H	Rotor Height	(m)
L	Reference Length	(m)
n	Number of Blades	
N	Revolution Per Minute	(RPM)
P	Power	(W)
R	Turbine Radius	(m)
t	Time Step	
T	Torque or Moment	(N.m)
λ	Tip Speed Ratio	
ρ	Air Density	(kg/m^3)
σ	Rotor Solidity	
ω	Angular Velocity	(Radians/Second)
v	Wind Velocity	(m/s)
ε	Turbulence energy dissipation per unit mass	(m^2/s^3)
μ	Dynamic viscosity	($N.s/m^2$)
k-ε	Turbulent model	
k-ω	Turbulent model	
μ	viscosity	(Ns/m^2)
μ_t	turbulent viscosity	(Ns/m^2)
τ	shear stress	(N/m^2)
α	angle	(degree)

List of Abbreviation

2D	Two-dimensional
CB-VAWT	Curved Blades VA
CFD	Computational Fluid Dynamics
COP	Coefficient of performance
DD	Dual rotor Darrieus Turbine
FEA	Finite Element Analysis
HAWT	Horizontal Axis Wind Turbines
IDMS	Improved-DMS
RANS	Reynolds Averaged Navier Stokes equations
SB-VAWT	Straight-Bladed Vertical Axis Wind Turbine
URANS	Unsteady Reynolds-averaged Navier-Stokes
VAWT	Vertical Axis Wind Turbine

CHAPTER ONE

INTRODUCTION

1.1 Introduction to Vertical Axis Wind Turbines

The thesis provides a comprehensive analysis of wind energy, covering both horizontal and vertical axis wind turbines, each having distinct configurations and operational characteristics. Horizontal axis wind turbines (HAWTs) are widely utilized and feature a horizontal rotor shaft with three blades rotating around a vertical axis. HAWTs outperform in high wind speeds, leveraging the blades' effectiveness in capturing wind energy. They are commonly deployed in large-scale wind farms with consistent wind resources. Their aerodynamic efficiency, streamlined shape, and adjustable blade pitch angles contribute to their efficient conversion of wind energy into mechanical energy.

On the other hand, vertical axis wind turbines (VAWTs) have a vertical rotor shaft, allowing the blades to rotate around this axis. VAWTs possess the advantage of capturing wind from any direction, making them suitable for sites with turbulent or variable wind patterns. VAWTs overcome challenges associated with HAWTs, such as wind direction tracking and yaw mechanisms. They perform well in lower wind speeds and provide consistent power generation in turbulent wind conditions. Their versatility makes them a viable option for a wide range of wind resource locations. Different types of wind turbine is shown in Figure 1.1 , The figure also shows the different types of wind turbines, their efficiency, and the differences between vertical and Horizontal wind turbines, where the Horizontal is more efficient, but with high cost, and The best type of VAWT is Darrieus VAWT, the highest in efficiency, and savonius VAWT is lowest Cp type and it works in low wind speed.

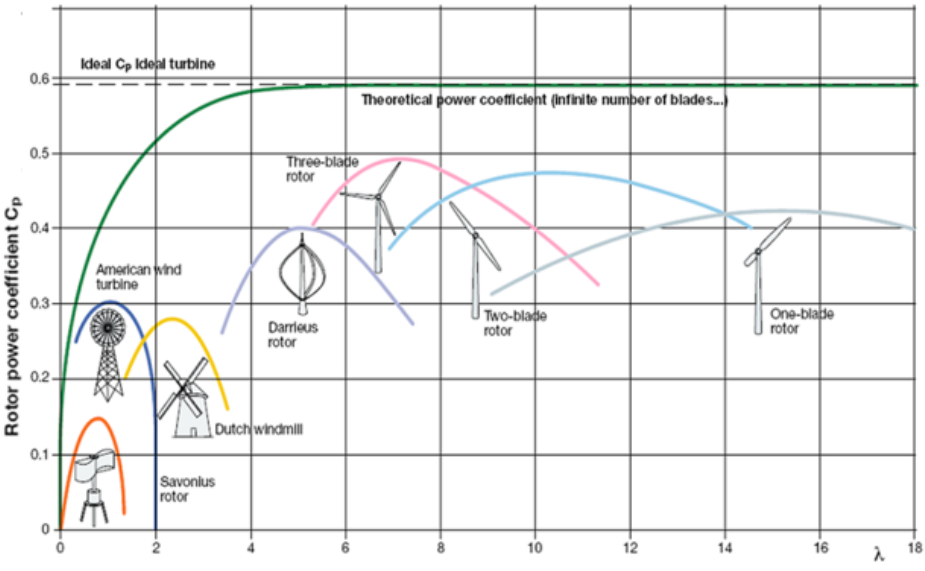

Figure 1.1 : Different Types of Wind Turbine

.

Among the various types of VAWTs, the thesis highlights the Darrieus and Savonius configurations. The Savonius turbine features a simple design with curved blades arranged in an "S" or "U" shape. Wind interacting with the blades induces rotor rotation through pressure differences. Savonius turbines are self-starting and perform efficiently in different wind conditions, including low-speed and turbulent winds. However, their overall efficiency is lower compared to other turbine types due to their reliance on drag-based operation.

On the other hand, the Darrieus turbine incorporates vertically aligned airfoil-shaped blades, forming a curved or "C" shaped rotor. Wind passing over the blades creates a pressure differential, leading to rotor rotation and energy generation. The Darrieus design excels in low wind speed conditions, offering superior starting torque and high efficiency. However, an external starting system is necessary to initiate rotation in Darrieus turbines.

The H-Darrieus turbine, or H-rotor, is a modified version of the Darrieus rotor where two sets of blades are symmetrically placed on either side of the vertical axis, forming an "H" shape. The H-Darrieus turbine offers improved stability and reduced unbalanced forces during operation compared to the traditional Darrieus rotor. This type of turbine exhibits enhanced structural integrity, reduced vibration, and potentially longer operational lifespan. The H-Darrieus configuration is particularly beneficial in applications where stability and structural considerations are critical, such as urban and building-integrated wind turbines [1]. Types of Wind Turbines Illustrated in Figure 1.2

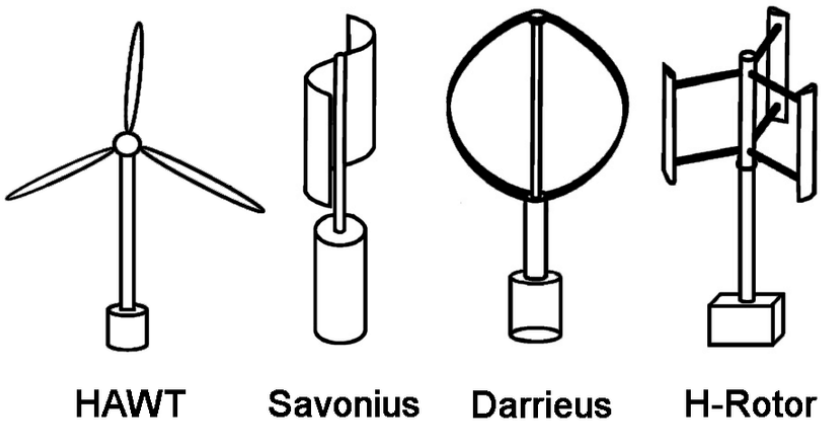

Figure 1.2: Types of Wind Turbines

1.2 Challenges of H-Darrieus Vertical Axis Wind Turbines

vertical axis wind turbines (VAWTs) face numerous obstacles that impact their performance and widespread acceptance. These challenges arise from the distinct design and operational characteristics of H-Darrieus turbines, which employ multiple blades arranged in an H shape around a central vertical axis.

A primary challenge revolves around aerodynamic efficiency, H-Darrieus VAWTs tend to exhibit lower aerodynamic efficiency when compared to alternative wind turbine designs like horizontal axis wind turbines (HAWTs). This discrepancy primarily arises from the complex flow patterns and blade interactions inherent in H-Darrieus turbines, resulting in increased drag and diminished power generation. Enhancing the aerodynamic efficiency of H-Darrieus VAWTs assumes paramount importance in improving their overall performance and competitiveness within the renewable energy sector.

Another challenge relates to structural stability and dynamic loading. The H-Darrieus configuration can engender heightened structural loads and vibrations during operation. The imbalanced forces acting on the blades can trigger oscillations and fatigue stresses, potentially compromising the structural integrity of the turbine. Addressing these dynamic loads and ensuring the long-term durability of H-Darrieus VAWTs necessitate meticulous design considerations and robust engineering solutions.

Furthermore, H-Darrieus VAWTs may encounter challenges concerning their starting and self-starting capabilities. Unlike HAWTs, which can rely on the wind's direction to initiate rotation, H-Darrieus turbines often require external mechanisms or power sources to overcome the initial torque. Establishing reliable and efficient self-starting mechanisms for H-Darrieus VAWTs remains an active research and development area.

The H-Darrieus configuration also poses challenges in terms of scalability and turbine size. As the number of blades increases in H-Darrieus VAWTs, so does the structural complexity and manufacturing costs. Scaling up the size of H-Darrieus turbines while preserving their performance and structural integrity becomes increasingly arduous, thereby limiting their deployment in larger capacity applications.

Additionally, VAWTs may face operational limitations under variable wind conditions. Their performance can be influenced by turbulent or fluctuating winds, resulting in reduced power output and augmented structural loads. Developing control strategies and adaptive mechanisms

to optimize the performance of H-Darrieus VAWTs in the face of variable wind conditions constitutes a significant research area within the realm of wind energy.

In summary, H-Darrieus VAWTs encounter challenges encompassing aerodynamic efficiency, structural stability, starting capabilities, scalability, and operational performance under variable wind conditions. Overcoming these challenges necessitates advancements in aerodynamic design, structural engineering, control systems, and the development of reliable self-starting mechanisms. By effectively addressing these challenges, researchers and engineers can bolster the performance and viability of H-Darrieus VAWTs, thereby facilitating the further integration of vertical axis wind turbines into the renewable energy landscape [1,2]

1.3 Objectives and Scope of the Study

The novelty of the presented study is to improve the overall Efficiency of wind turbines. This involves identifying and developing designs that can maximize the Efficiency. The present study has been undertaken with the following objectives:

- Examine single blades vertical axis wind turbines through both numerical and experimental methods, followed by a comparative analysis.
- Explore the impact of a dual-blade configuration using both numerical and experimental approaches.
- Studying the effects of different factors such as location of the Second blades and wind speed on the Power coefficient.

Comparing the results of Power coefficient between the single and the Double blade.

1.4 Organization of the Thesis

The thesis is divided into five chapters, chapter one introduction for thesis then the background theories and concepts related to the present research work are discussed in chapter two, chapter three, titled "chapter three: experimental model and numerical model" begins with introduction to experimental model, experimental setup then numerical model, introduction to numerical simulation, overview of the turbine and data, meshing, solver setting sand summary.

chapter four, titled "chapter four: results and discussion" is divided into two sections: results and discussion. the results section focuses on the outcomes of the research, specifically examining the performance of both single and double blade Darrieus VAWTs. within the results section, the experimental and numerical (1.1), (1.2) results for single and double blade configurations are presented separately.

finally, chapter five, titled "chapter five: conclusion and future works" provides a comprehensive summary of the thesis's main findings and conclusions drawn from the research. additionally, this chapter presents suggestions for future research and areas of further investigation to enhance the understanding and development of H-Darrieus VAWTs.

in this manner, the organization of the thesis ensures a systematic and logical progression of the research, allowing readers to follow the study's objectives, methodologies, findings, and implications in a cohesive and structured manner.

CHAPTER TWO

LITERATURE SURVEY

2.1. Introduction

Wind energy has grown in the past decade as a renewable energy source after solar energy. Wind turbine is a kind of rotating machinery. Horizontal Axis Wind Turbines (HAWT) is preferred for multi-Megawatt power. However, the Vertical Axis Wind Turbine (VAWT) with the main advantages of structural simplicity, withstand high turbulence winds, cost effectiveness, easier maintenance, and lower noise emission receives more and more attention in small-scale wind power market. They can be installed in low wind speed regime for performing various small-scale functions ranging from electrifying a built environment to pumping water especially in remote places where grid connected electricity is a scarce. The Straight-Bladed VAWT (SB-VAWT) is one of the most researched and studied VAWTs.

Bošnjaković et al. [3] indicated a review of available literature based on upscaling wind turbines and minor design improvements. That review included further improvements in rotor blade aerodynamics, active control of the rotor blade rotation system, and aerodynamic brakes that would lead to increased power generation efficiency. **Li [4]** reviewed the historical development of the SB-VAWT briefly. Then they introduced the aerodynamic models for the turbine design and performance analysis. Finally, they presented the types of traditional and new SB-VAWT and their characteristics and main utilizations. **Kumar et al. [5]** intended to summarize the development of VAWT, in particular, Darrieus turbine from the past to the project that is underway. They discussed the reason for the technical challenges and past failures. Moreover, they assessed various configurations of VAWT in terms of reliability, components and low wind speed performance. They investigated innovative concepts and the feasibility to scale up for megawatt electricity generation, especially in offshore environments. They proposed that review as an information hub for the major developments in VAWT and its technical advancements. **Ghasemian et al. [6]** reviewed published works on CFD (computational fluid dynamic) simulations of Darrieus VAWTs. They presented recommendations and guidelines for turbulence modeling, spatial and temporal discretization, numerical schemes and algorithms, and computational domain size. They investigated the operating and geometrical parameters such as tip speed ratio, wind speed, solidity, blade number and blade shapes. Their purpose was to address different progresses in simulations areas such as blade profile modification and optimization, wind turbine performance

augmentation using guide vanes, wind turbine wake interaction in wind farms, wind turbine aerodynamic noise reduction, dynamic stall control, self-starting characteristics, and effects of unsteady and skewed wind conditions.

Darrieus VAWTs have been recently identified as the most promising solution for new types of applications. For that, these turbines are experiencing renewed interest from researchers and manufacturers**. Islam et al. [7]** collected the main aerodynamic models that had been used for performance prediction and design of straight-bladed Darrieus-type VAWT in a review. They found that the most widely used models were the Double-Multiple Stream Tube model (DMST), Vortex model and the Cascade model. However, they discussed strengths and weaknesses of each of those three models. **Bangga et al. [8]** conducted assessments by employing the (DMS), Improved-DMS (IDMS), Unsteady Blade Element Momentum (UBEM), Vortex Model and fully resolved (CFD) approaches. They used three different codes; FLOWer, TAU and Ansys Fluent. Their studies demonstrated that there was consistent agreement between engineering models at lightly loaded cases for the power curve prediction. They declared that discrepancy at high tip speed ratio (λ) (TSR) was caused by wake expansion, unsteady and de-cambering effects. In contrast, CFD hardly showed consistent power prediction but delivered accurate thrust values. Moreover, **Beri and Yao [9]** applied (DSMT) model for the performance prediction of straight bladed fixed pitch VAWT using NACA0018 airfoil at low wind speed. They used a moving mesh technique to investigate two-dimensional unsteady flow around the same VAWT model with a modified NACA0018 airfoil. It was flexible at 15˚ from the main blade axis of the turbine at the trailing edge located about 70% of the blade chord length. They used Fluent solving Reynolds average Navier-strokes equation. Their results from Double-Multiple-Stream tube model and the simulation results were compared and showed that the CFD simulation with airfoil modified had better performance at low tip speed ratios. **Brusca et al. [10]** analyzed the link between the aspect ratio of a vertical-axis straight-bladed (H-Rotor) wind turbine and its performance (power coefficient). Since the aspect ratio variations of a vertical-axis wind turbine cause Reynolds number variations, any changes in the power coefficient can also be studied to derive how aspect ratio variations affect turbine performance. Using a calculation code based on the Multiple Stream Tube Model, symmetrical straight-bladed wind turbine performance was evaluated as aspect ratio varied. Their numerical analysis highlighted how turbine performance is strongly influenced by the

Reynolds number of the rotor blade. From a geometrical point of view, as aspect ratio falls, the Reynolds number rises which improves wind turbine performance.

Jekabsons et al. [11] focused on numerical and experimental studies on the aerodynamic performance of the straight-bladed Darrieus type turbine. They evaluated the characteristic parameters for practically applicable turbine designs using (CFD) tools. They used the Unsteady Reynolds-averaged Navier Stokes approach in two- and three-dimensional turbulent flow computations around the VAWT with the extended version of the open sourced CFD toolkit Open FOAM. They investigated numerically several constructions of three or six-blade symmetric NACA0015 airfoils. Rotation of the wind turbine rotor has been realized by Generalized Grid Interface (GGI). It uses weighted interpolation to evaluate and transmit the flow values across a pair of conformal or non-conformal coupled boundaries between the stationary and rotating domains. **Bianchini et al. [12]** suggested a more in depth understanding of the physical phenomena that govern the aerodynamics past a rotating Darrieus turbine was needed to improve their efficiencies further and make them competitive with those of conventional HAWT. Due to the complexity of similar simulations, however, the possibility of having reliable and detailed experimental data to be used as validation test cases was pivotal to tune the numerical tools. They applied a two-dimensional U-RANS computational model to analyze the wake characteristics on the mid plane of a small-size H-shaped Darrieus VAWT. Also, they tested the turbine in a large-scale, open-jet wind tunnel, including both performance and wake measurements. Good agreement on the turbine performance estimation was constantly appreciated between simulations and experiments along the structure of the wake and the main macro-structures of the flow to the local aerodynamic features of the airfoils in cycloidal motion. Moreover, **Bianchini et al. [12]** used a unique tow tank experimental data on the performance curve and the near-wake structure of a Darrieus rotor as a benchmark to validate the effectiveness of different CFD approaches. In particular, a dedicated analysis was provided to assess the suitability, the effectiveness and the future prospects of simplified two-dimensional (2D) simulations. They discussed the correct definition of the computational domain, the selection of the turbulence models and the correction of simulated data for the parasitic torque components. Their results clearly show that, (only) if properly set, two-dimensional CFD simulations are able to provide - with a reasonable computational cost - an accurate estimation of the turbine performance and also quite reliably describe the attended flow-field around the rotor and its wake. Also by ANSYS CFX software, **Cai et al. [13]** simulated the H-Rotor VAWTs with and without winglets based on structured meshing

technology and incompressible continuity Reynolds Averaged Navier Stokes equations (RANS) solver. Their CFD and experimental results of the rotor power coefficient had a good agreement during the range of calculations. The rotor output torque and power coefficient of H-type VAWT with winglets is 10% to 19% higher than that of the original H-type VAWT. The maximum torque increased by 12.8% and the negative torque was avoided when tip ratio reached 1.53; the minimum and maximum thrust increased by 26.7% and 3.4%, respectively. The vorticity distributions at the tips of winglet H-Rotor blades were weaker than the H-Rotor without winglets. The aerodynamic performance of the near region of blade tips was improved. Winglets increased the overall torque-generating. Their results provided a valuable reference or benchmark for the design and optimization of future winglet H-Rotor VAWTs.

For wind turbine solidity, **Bangga et al. [8]** selected three different turbines from low up to higH-Darrieus solidity (0.23, 0.53 and 1.325) as the case studies. They declared that as solidity increased, coefficient of power decreased. **Singh et al. [14]** suggested a solution for non-self-starting characteristics by replacing its conventional blades with increasing rotor solidity. However, there was still hardly any quantitative measure of the self-starting, torque, power coefficient etc. with increased rotor solidity (from 0.8 to 1.2) so as to obtain some performance insights of high solidity unsymmetrical blade H-Darrieus rotor in low wind speed condition. The authors evaluated the power coefficients (Cp) at various wind speeds. They showed that high blade solidity was in fact desirable for overall better performance of the rotor and an optimum rotor solidity at which power coefficient is the highest. A maximum Cp of 0.32 was obtained for rotor solidity 1.0 and wind speed 5.7 m/s. Moreover, **Soultanzadeh and Moradi [15]** mentioned the same point that increasing the solidity in VAWT leaded to decreasing coefficient of performance (COP) despite the improved start-up performance. To overcome that problem, **they [15]** proposed the pitch regulation system for increasing the solidity. They tested the effect of pitch angle on low solidity VAWT at uniform flow conditions and low turbulence intensity in wind tunnel test sections (not real conditions). They investigated numerically and experimentally under realistic condition the influence of pitch angle on the aerodynamic performance of a small Darrieus-type straight-bladed high-solidity VAWT equipped with a pitch regulation system. The COP was measured and calculated at different tip speed ratios and two pitch angles of 0 and 5°. The results reveal 25% enhancement in maximum COP with the increase of pitch angle up to 5°. They found that increasing the pitch angle at a constant tip speed ratio is followed by accelerated vorticity generation, occurrence

of maximum COP at lower tip speed ratio and smoother velocity profile in lateral distances of the rotor. **Firdaus et al. [16]** presented a numerical simulation and experiment on the effect of the variable pitch angle on the performance of a small Vertical-Axis Wind Turbine (VAWT) with straight blades. They experimentally measured the power coefficient in an open-circuit wind tunnel. However, they numerically conducted two-dimensional unsteady computational fluid dynamics simulations using the RNG k-ε, Realizable k-ε, and SST k-ω models and analyzed the power and torque of the VAWT and the flow around the straight blades. They validated numerical simulation using wind tunnel experimental data. Their results showed that a VAWT with variable-pitch blades had better performance than a VAWT with fixed-pitch blades.

Savonius type Small (SVAWT) are cheap, simple in construction, self-starting, Omni-directional, less noise, requires no yaw mechanism to continuously orient towards the wind direction. Savonius wind turbines are workable in low wind speed regimes. It can be fitted on rooftops and also suitable for the urban areas. **Gaikwad et al. [17]** made a review on the Savonius VAWT and introduced the diverse surveys related with Savonious rotor plan and its stability. They assumed cutting edges as a fundamental part in the exhibition of vertical hub wind turbine. The energy extracted from twist regarding distinctive outline parameters was additionally displayed in their review. Their work focused on the utilized of existing writing for building up the low breeze speed twist generators with enhance the execution of Savonius rotor. Furthermore, **Kadam and Patil [18]** reviewed Savonius wind rotors and identified its performance parameters to increase its power performance. They concluded that two-blade rotor was more stable in operation than three or more rotor blades. Power coefficient increases with increasing the aspect ratio. The rotor blades with end plates give higher efficiency than those of without end plates. **Roy and Saha [19]** presented an unsteady two-dimensional computational study in order to observe the effect of overlap ratios on static torque characteristics of a VAWT. Their study was performed with the help of a finite volume based on CFD software package Fluent 6.3. The computational model was a two-bladed conventional VAWT having overlap ratios of 0, 0.10, 0.15, 0.20, 0.25 and 0.30. They started a comparative analysis by using various k-turbulence models and compared their results with the experimental data available in literature. They found that a realizable k-turbulence model with enhanced wall treatment suitable for further computational analysis. Also, they studied the flow field around the turbine model with the help of static pressure contour analysis. They realized that an overlap

ratio of 0.20 eliminates the effects of negative static torque coefficient, provides a low static torque variation at different turbine angular positions and also gave a higher mean static torque coefficient as compared to the other overlap ratios. **Ali [20]** studied experimentally the performance of Savonius wind turbine made a comparison between two and three blades. Those blades were semi-cylindrical fabricated from Aluminum sheet with aspect ratio of one where Savonius wind turbine has its maximum performance and a high starting torque. They observed that two blades Savonius turbine was more efficient with a higher power coefficient. They gave a reason that increasing the number of blades would increase the drag surfaces against the wind air flow and caused an increase in the reverse torque and a decrease in the net torque. Besides, **Mahmoud et al. [21]** experimentally studied different geometries of Savonius wind turbine in order to determine the most effective operation parameters. They found that two-blade rotor was more efficient than three and four ones. The rotor with end plates gave higher efficiency than those of without end plates. Double stage rotors had higher performance compared to single stage rotors. The rotors without overlap ratio were better in operation than those with overlap. Their results showed also that the power coefficient increases with rising the aspect ratio. **Sawla et al. [22]** numerically studied the performance of Savonius turbine (Air inlet velocity = 4 m/s, aspect ratio = 1.45 and overlap ratio = zero) using Ansys 14.0 CFX. Pressure, velocity and Turbulence Kinetic Energy Analysis were performed at different attack Angle. **Widodo et al. [23]** computationally presented the design and analysis of the Savonius rotor blade to generate 5 kW power output. They studied the relevant design parameters and theories and used them to determine related design geometry and requirements of the Savonius rotor blade (diameter of 3.5 m and rotor height of 7 m). The three-dimensional model of Savonius rotor blade was created by using SolidWorks software. They presented (CFD) analysis and structural Finite Element Analysis (FEA). CFD analysis was performed to obtain the pressure difference between concave and convex region of the blade while FEA was done to obtain the structural response of the blade due to the wind load applied in term of stresses and its displacements. **Dobrev and Massouh [24]** studied the flow through Savonius wind turbine (aspect ratio of 1). It was intended to be used within a compact package with multisource of energy. They performed three-dimensional simulation of flow through the wind turbine to observe strong unsteady effects including separation and vortex shedding. They permitted the turbulence modeling by means of k-Z and DES to obtain good results comparatively to experiments. Moreover, they used CFD to study the behaviour of a Savonius wind turbine under flow field conditions and to determine its performance and the evolution of wake geometry. The flow analysis helped to qualify the design of the wind turbine.

Experimental investigation in wind tunnel was carried out using PIV to validate simulations. Their investigation permitted to determine the structure of the real flow and to access the quality of numerical simulations.

Savonius turbine's efficiency is only in the range of 15%-21%. Investigations are being conducted to improve its efficiency by controlling its design parameters. **Sharma et al [25]** investigated the performance of a two-stage two-blade configuration of the Savonius rotor. They experimentally studied overlap, tip speed ratio, power coefficient (Cp) and torque coefficient (Ct). They optimized overlap ratio of the design to generate maximum performance of the rotor. They showed that at 9.37% overlap condition a maximum Cp of 0.517 was obtained, which was much higher than the conventional Savonius rotor. Furthermore to improve the performance of the Savonius rotor, **Maldonado et al. [26]** investigated a detailed study of Savonius wind rotor in order to obtain the optimal characteristics. They developed designed Savonius wind rotor assembly on CAD software and the simulations of the interaction between the flow of air and blades through finite element analysis. They showed the velocity distribution of the profile blades and the pressure profile due the velocities profiles. They also studied vortices formations. They simulated blades with different geometry and gap distance between the blades to improve the (Cp) which increased about 20%. The wind was directed through gap distance between the blades to the surface of following blade to induce its rotation. An air deflector was located front the Savonius rotor to increase and guide the flow of air to the blades. The deflector increased the velocity of the Savonius rotor up to 32%. From the simulation results, a Savonius wind rotor prototype was built at scale 2:1. Field tests were performed to check the amount of energy obtained with the changes implemented. **Irabu and Roy [27]** experimentally investigated to improve and adjust the output power of Savonius rotor under various wind power and suggested a method of prevention the rotor from strong wind disaster using a guide-box tunnel. The area ratio between the inlet and exit of it was variable to adjust the inlet mass flow rate or input power. They conducted experiments to find an adequate configuration that provided the best relative performance. Their experiment didn't include the test of strong wind. Their experiments included the static torque test of the fixed rotor at any phase angle and the dynamic torque test at rotation of them. Consequently, they found the maximum rotor rotational speed in the range of the guide-box area ratio between 0.3 and 0.7. At area ratio of 0.43, the output power coefficient increased about 1.5 times with three blades and 1.23 times with two blades greater than that without guide-box tunnel, respectively.

It seemed that the performance of Savonius rotor within the guide-box tunnel was comparable enough with other methods for augmentation and control of the output.

Hydropower from the river is one of the best renewable sources. Hydropower source is predictable compared to wind or solar energy. For generation of electricity using the kinetic energy of natural water resources, Savonius rotor is one of the best types of turbine. The Savonius turbine is more popular as wind turbine. However, attempt is made for use of Savonius rotor as hydro-turbine application. **Patel C.R et al. [28]** built and analyzed a three-dimensional computational model using a (CFD) analysis using ANSYS. They investigated the effect of overlap ratio for performance enhancement Savonius turbine. They studied three different overlap ratios, 0.0, 0.1 and 0.2, at different angular speeds of rotor. They found that the maximum torque can be obtained at overlap ratio of 0.2. For hydrokinetic turbines of Savonius, **Wahyudi et al. [29]** numerically studied their performance using a Tandem Blade Savonius (TBS) rotor (three types: overlap, symmetrically and convergence). They identified the influenced parameters and showed that the optimum efficiency of the Savonius rotor could be improved their partition space between blade and tandem. Their simulation showed the way of the flow characteristic and pressure distribution pattern in and around of the blade swept area. Their results showed that the convergence TBS (convergence) had a higher gap pressure between upstream and downstream and they had best performance than other two types.

For Cambered Blades, **Rainbird et al. [30]** recommended a better understanding of Darrieus turbine aerodynamics to improve their designs; e.g. blade element momentum models. They mentioned that many of these models neglected the impact of the curved paths that were followed by blades on their performance (curved streamlines of the flow). They conducted wind tunnel experiments to obtain lift and drag for three airfoils: a NACA 0018 and two conformal transforms of the profile. When transformed airfoils were used in a Darrieus turbine with blade chord-to-turbine radius ratios, c/R, of 0.114 and 0.25, a parallel computational fluid dynamics campaign were conducted to study the aerodynamic behavior of the same blades in curvilinear flow in Darrieus-like motion. Besides, they calculated turbine performance using computational fluid dynamics and a blade element momentum code, for each of the blades in turn. Their computational fluid dynamics results for the NACA 0018 agreed closely to blade element momentum results for the equivalent cambered airfoil where c/R = 0.25, for both

turbine power and blade tangential forces. When they modeled a Darrieus rotor using blade element momentum methods and applied experimental data for the used profile, they concluded that the turbine would yield inaccurately if the c/R ratio is high. In such cases, it was necessary to select a profile based on the virtual shape of the blades. In Thailand, **Chaichana et al. [31]** studied the effect of the operating conditions (TSR) to start rotation, increase rotation, power and torque coefficients of Curved Blades VAWT(CB-VAWT). It was experimentally tested in wind tunnel with setting velocities of 1.5, 2.0, 3.0, 4.0 and 5.0 m/s. Four identical blades of semi-cylindrical hollowed drum shape were the main essential parts of CB-VAWT. The swept diameter of turbine was set at 300 mm^2. The analysis of the experimental results showed that when the shaft was locked (rotational speeds of CB-VAWT become is zero), a maximum tangential force existed at the torque-pulley. Cut in wind speed increase corresponding to the increasing of tangential force ratio. The increase of rotation period depended on wind speed and tangential force ratio. The required time of rotor to accelerate from starting up to reach the rated rotational speed was relative to the increase of tangential force ratio and/or decreasing of wind speed. Their optimal tip speed ratio to create a maximum power coefficient was within the range of 1.5 to 2.5. The power coefficient of CB-VAWT reached value of about 5 – 7.5%. However, at a constant wind speed, torque coefficient reduced with an increasing of the tip speed ratio. **Matrawy et al. [32**] presented an experimental study for the main design and performance parameters concerning by a small scale VAWT. Two models (Two and Four cambered blades) were designed and tested in an open wind tunnel. Their studied parameters were variation of rotational speed at different blade angles, variation of torque and power coefficients at different tip speed ratios. They also investigated the performance of VAWT with/without leading edge flap blades. They presented their experimental data at different blade angles ranges from 15^o to 60^o in order to give an acceptable blade angle. A simple theoretical model was developed to verify and checkup some experimental results. The final experimental results showed that the blade angle of 45^o enhances the performance of VAWT comparing the other ones for both two and four bladed rotors. Furthermore, using a flap blade enhances the maximum power coefficient by 2.4% compared by the same model without flap blade. **Loya et al. [33]** numerically investigated the dependency of torque on Darrieus turbine with aerofoil with fixed pitch blades. They generated coordinate points for aerofoil using Java Foil software. They used (RANS) turbulence modelling for predicting the flow and efficiency. They considered unsteady flow condition to make simulation as realistic as possible. In order to visualize high strain flow and separation, they used two-equation model k-ε with RNG. They used NACA 0012 aerofoil and carried out camber variations for developing samples of aerofoil

to check the enhancement in performance of VAWT. They investigated that the performance efficiency was significantly improved by changing the aerofoil camber, demonstrating the highest torque and the least performance. Zidane et al. [19] study Enhancing H-Darrieus VAWT performance by using upstream deflectors. Investigated deflector configurations and compared turbine performance with and without wind rotor barriers. Validated CFD models provided novel insights on deflector effects. Provided that the Single deflector increased moment coefficient by 24%, two deflectors increased it by 22% within optimal tip speed ratio range.

For new models and configurations, **Bashar [35]** improved the design and performance of VAWT to make it more attractive, efficient, durable and sustainable. They mentioned that airfoil has some good aerodynamic characteristics match with the characteristics of Savonius type VAWT; such as good stall characteristics, little roughness effect, relatively high drag and low lift coefficients. They designed three-Dimensional CAD models using Solidworks and performed CFD simulation for five different VAWT designed models. Then, they developed moving mesh and fluid flow simulation using FLUENT. Their simulations results provided pressure contour, velocity contour, drag coefficient, lift coefficient, torque coefficient and power coefficient. Physical models of NACA5510, NACA7510 and semicircular rotors of three bladed are fabricated and tested in subsonic wind tunnel. They experimentally measured dynamic torque using dynamic torque sensors for all these models at three different speeds. By comparing the numerical and experimental results, they concluded that NACA7510 air foiled VAWT model gave the better performance at higher Tip Speed Ratio than other two models. However, **Howell et al. [36]** provided a combined experimental and computational learn about aerodynamics and overall performance of a small scale VAWT. They generated two- and three-dimensional unsteady CFD models to help understand the aerodynamics performance. They carried out wind tunnel checks to verify usual performance of the turbine. Also, they introduced wind tunnel overall performance effects for instances of characteristic wind velocity, tip-speed ratio, solidity and rotor blade surface finish. They experimentally proved that the floor roughness on the turbine rotor blades had a vast effect on performance. Below a crucial wind speed ($Re = 3 \times 10^4$), the overall performance of the turbine was degraded via a clean rotor floor end, but above it the turbine overall performance was improved by an easy floor finish. They tested two- and three-blade rotors and revealed the overall performance coefficient for the greater solidity rotors for the three-blade rotors over most of the running range. They proved

dynamic stalling behavior and the resulting massive and speedy changes in pressure coefficients and the rotor torque to be the in all likelihood cause of modifications to rotor pitch attitude that came about at some stage in early testing. The overall performance coefficient estimated by the two-dimensional computational was significantly higher than that of the experimental and the three-dimensional CFD model. Their predictions showed that the presence of the over tip vortices in the three-dimensional simulations was responsible for producing the large distinction in efficiency compared to the two-dimensional predictions. They explored dynamic behavior of the over tip vortex as a rotor blade rotates via every revolution. **Rahman et al. [37]** compared performances of different VAWT models using both numerical and experimental methods to find the one with the optimum performance. Standard aero-foil blade designs were considered because of their good aerodynamic characteristics. The two-dimensional CAD design of different VAWT models including aero-foil blades (i.e. NACA5510, NACA7510 and NACA9510) were performed using Solid Works. The authors performed CFD simulation of wind flow around these models using FLUENT and the moving mesh technique. They obtained pressure and velocity contours and lift coefficient, drag coefficient, torque coefficient and power coefficient for all models. They fabricated and experimentally tested physical models of NACA 7510, NACA 5510 and semicircular VAWTs in a subsonic wind tunnel at three different speeds to measure dynamic torques. Their study showed that the VAWT model with NACA 7510 blade produced the best result among all the models at a relatively high Tip Speed Ratio (TSR). Moreover, **Rahman et al. [38]** numerically and experimentally analyzed six different rotor plans and proposed models incorporate a conventional Savonius with two different edges criteria and 90^{o} degree helical bend models with two, three and four sharp edges. They designed the models using SolidWorks then the physical models were 3D printed for testing. Their helical models with two and three cutting edges have the best self-starting ability in low wind speeds. Helical VAWT with three edges started revolution of 35 rpm at only 1.4 m/s wind speed under no generator stacking. Their most noteworthy power coefficient was accomplished by the helical VAWT with two sharp edges. **Alaimo et al. [39]** analyzed the complex and unsteady aerodynamic flow related with wind turbine. They studied the effect on exclusive numerical aspects on the accuracy of simulating a rotating wind turbine. In particular, their results of mesh dimension and structure, time step and rotational velocity had been taken into account for simulation of distinctive wind turbine geometries. They evaluated the performance between a straight blade VAWT and a helical blade one. Analyses were carried out using Computational Fluid Dynamic ANSYS Fluent software, fixing the Reynolds averaged Navier–Stokes (RANS) equations. They used

two-dimensional simulations in a preliminary setup of the numerical manner and to compute approximated performance parameters, specifically the torque, power, elevate and drag coefficients. Then, three-dimensional simulations were carried out. The authors stated static and dynamic consequences for characteristic values of rotational speed.

Parker and Leftwich [40] visualized the flow surrounding a scaled model (VAWT) at realistic operating conditions. The model closely matches geometric and dynamic properties of (TSR) and Reynolds number. They visualized the flow using particle imaging velocimetry (PIV) in the midplane upstream, around, and after (up to 4 turbine diameters downstream) the turbine, as well as a vertical plane behind the turbine. Their results showed that the wake structure is much more sensitive to changes in Tip Speed Ratio than to changes in Reynolds number. Time-averaged results showed an asymmetric wake behind the turbine with a larger velocity deficit for a higher (TSR). For the higher tip speed ratio, an area of averaged flow reversal was present with a maximum reverse flow of $0.04U_{\infty}$. Phase-averaged vorticity fields showed distinct structures form from each turbine blade. There were distinct differences in results by Tip Speed Ratios of 0.9, 1.3 and 2.2 of when in the cycle structures were shed into the wake, switching from two pairs to a single pair of vortices being shed. **Rezaeiha et al. [41]** mentioned that accurate prediction of the performance of a (VAWT) using (CFD) simulation required a large domain size enough to minimize the effects of blockage and uncertainties in the boundary conditions on the results. It also required the employment of a sufficiently fine azimuthal increment combined with a grid size at which essential flow characteristics could be accurately resolved. They systematically investigated the effect of the domain size and azimuthal increment on the performance of a two-blade VAWT operating at a moderate tip speed ratio of 4.5 using two-dimensional with the (URANS). They studied the grid dependence of their results using three systematically refined grids. Their turbine had a low solidity of 0.12 and a swept area of 1 m^2. Refining azimuthal increment from 10.0 to 0.5 resulted in a significant increase in the predicted power coefficient while the effect was negligible with further refinement from 0.5 to 0.05. Furthermore, a distance from the turbine center to the domain inlet and outlet of 10D each, a domain width of 20D and a diameter of the rotating core of 1.5D were found to be safe choices to minimize the effects of blockage and uncertainty in the boundary conditions on the results. Moreover, **Rezaeiha et al. [42]** mentioned that the accuracy of CFD simulations of (VAWTs) was significantly associated with the computational parameters, such as azimuthal increment, domain size and number of turbine revolutions before

reaching a statistically steady state condition (convergence). They prepared a detailed review of the literature, however, indicated that there was a lack of extensive parametric studies investigating the impact of the computational parameters. Therefore, they intended to systematically investigate the impact of these parameters on the simulation results at different Tip Speed Ratios and solidities. The evaluation was based on CFD simulations validated with wind tunnel measurements for two VAWTs. Instantaneous moment coefficient and power coefficient were studied for each case using (URANS) simulations with the four-equation transition SST turbulence model. Their results showed that the azimuthal increment was largely dependent on Tip Speed Ratio. The need for finer time steps was associated to the flow complexities related to dynamic stall on turbine blades and blade-wake interactions at low TSR. In addition, the minimum distance from the turbine center to the domain inlet and outlet was 15 and 10 times the turbine diameter, respectively. Their current findings can serve as guidelines towards accurate and reliable CFD simulations of VAWTs at different tip speed ratios and solidities.

The practice of reproducing wind tunnel tests by means of CFD numerical simulations (Numerical Wind Tunnel (NWT)) is becoming quite common in many research fields of wind engineering. Wind tunnel tests can provide the crucial validation data needed for CFD numerical simulations. **Burlando et al. [43]** applied Numerical Wind Tunnel technique to study the flow around and inside a multi-stage VAWT surrounded by stator vanes. First, they experimentally studied the flow field in the wind tunnel. Then, they used the experimental results to validate a CFD model. They finally used numerical model to study and describe how the results obtained by means of the physical model can be extended to more general conditions. To improve wind farms' performance and reliability, **Smily and Radi [44]** presented good modeling of the air flow around a wind turbine blade profile by introducing random parameters relating to the fluid. They first numerically presented S809 airfoil validation using ANSYS CFX by comparing the pressure coefficients, calculated for different turbulence models, with experimental data. Then, they introduced the uncertainties to determine the influence of the input variables on the aerodynamic output coefficients. The performance augmentation of pairs of VAWTs is known to be dependent on incident wind direction, turbine spacing and direction of rotation. However, there is a lack of robust numerical models investigating the impact of these parameters. **Hansen et al. [45]** performed two-dimensional CFD simulations of an isolated VAWT and of co- and counter-rotating pairs of

VAWTs with the aim to determine turbine layouts that can increase the power output of VAW farms. They conducted a lot of simulations at a turbine diameter Reynolds number of $1.35x10^7$. Also, they conducted a mesh convergence study and investigated the influence of mesh size, domain size, azimuth increment, number of iterations per time step, and domain cell density. Their results showed that mesh size, domain size and azimuth increment proved to have the biggest impact on the converged results. For the configurations analysed, pairs of VAWTs exhibited a 15% increase in power output compared to operating in isolation, when the second rotor was spaced three turbine diameters downstream and at an angle of to the wind direction. Furthermore, when three turbines were positioned in series, the power output was greater than a pair by an additional 3%.

In Iraq, **Altmimi et al. [46]** presented the full details of design for VAWT and how to find the optimal values of necessary factors. Additionally, the results shed light on the efficiency and performance of the VAWT under different working conditions. It was taken into consideration the variety of surrounding environmental conditions (such as density and viscosity of fluid, number of elements of the blade, etc.) to simulate the working of vertical wind turbines under different working conditions. Furthermore, the effect of the design factors was investigated such as the number and size of the blades on the behavior and performance of VAWT. QBlade software was used to achieve the calculations and optimization processes to obtain the optimal design of vertical axis wind turbines that was suitable for the promising sites. In Thailand, **Unsakul et al. [47]** presented effects of design factors on mechanical performance of (VAWTs). They experimentally investigated the optimal VAWT performance under low wind speed conditions. Design factors included types of wind turbines, number of blades, types of materials, height-to-radius ratios and design modifications. Moreover, they numerically analyzed the potential VAWT models with different design factors within a virtual wind tunnel at various wind speeds by utilizing XflowTM (CFD) software. They obtained the performance curves of each VAWT as plots of power coefficients against tip speed ratios. They found that the type of wind turbine, number of blades, and height-to-radius ratio had significant effects on mechanical performance whereas types of materials result in shifts of operating speeds of VAWTs. Therefore, they developed an optimal VAWT prototype to operate under actual low speed wind conditions. The performance curve from experimental results agreed with the CFD results.

H-type Darrieus rotor has become more popular in the built environment for their straight blade designs and simpler construction features; however, their major problem is their non-self-starting characteristics. Self-started capability "starting behaviour" is an essential feature to obtain less difficult and more cost-effective turbines. **Rossetti and Pavesi [48]** introduced and compared different processes to describe the self-start of an H-blade Darrieus rotor. They accomplished two- and three-dimensional CFD simulations. The (TSR) versus power coefficient curves and the growth of the trust forces over a blade revolution highlighted the limits and the strengths of each approach. The BEM model showed remarkable limits to describe the self-start behavior of the tested geometry. The principal limits of the BEM approach were recognized to the absence of well documented aerofoil databases for low Reynolds number and the inadequate modelling of dynamics effects. Their two-dimensional simulation allowed highlighting the unsteady features of the flow fields, and the presence of a complex vortices pattern which interact with the blade. Furthermore, the comparison between two- and three-dimensional data demonstrated the importance of three-dimensional effects such as secondary flows and tip effects, which had a positive effect on start-up, increasing the torque characteristic for TSR of 1. The start-up capability of H-Darrieus appears to be influenced by many different factors, which include secondary flows, three-dimensional aerodynamic effects and the finite aspect-ratio of the blades. **Singh et al. [14] d**eclared that H-type Darrieus rotor has non-self-starting characteristics due to symmetrical blade designs. The authors investigated a three-bladed H-type Darrieus rotor equipped with unsymmetrical S1210 blades at various azimuthal positions and evaluated the power coefficients at various wind speeds. Their results were compared with some other symmetrical/unsymmetrical blade H-Darrieus rotors. The operating range was reduced for higher static and dynamic torque and comparable power coefficient with respect to existing rotors. Their rotor could be used for various small-scale applications. Also, **Asr et al. [49]** investigated the start-up behavior associated with Darrieus turbines. A series of transient CFD simulations were carried out using ANSYS Fluent. In their work, the turbine was left free to accelerate based on the torque experienced over time. Careful considerations were made with regarding to turbulence modeling and grid generation to ensure investigation accuracy. Their method yielded a high level of accuracy, proving its usefulness for similar problems after validated with the published experimental data. Their CFD setup evaluated the effects of several geometric characteristics of the turbine rotor on the starting characteristics. They observed the optimum start-up

characteristics with the use of a medium-thickness cambered airfoil, NACA2418, put to use with an outward pitch angle of 1.5. That configuration decreased the start-up time while retaining the turbine's peak performance. Moreover, **Celik et al. [50]** built a CFD start-up model after conducting a research to evaluate the self-starting behavior of the H-type VAWT. The self-starting behavior of a VAWT was used for validation, and then the important points of aerodynamics of the start-up system had been examined. They analyzed the influence of the moment of inertia and the blade variety on the aerodynamic behavior of the self-starting and power performance of the H-type VAWT. Their results showed that increasing inertia of the turbine demonstrated no practical effect on the turbine start-up behavior and closing rotational speed. However, an increase in the instantaneous turbine electricity all through the start-up method after the finest TSR was foud with decreasing the turbine inertia. They concluded that increasing the blade range made the turbine simpler to start-up. **Untaroiu et al. [51]** undertook a systematic evaluation of (VAWT), starting with establishment of a methodology for VAWT simulation. Replicating the experimental prototype, they generated each two-dimensional and three-dimensional models of a three-blade VAWT. Full transient (CFD) simulations and mesh deformation functionality reachable in ANSYS-CFX had been run from turbine start-up to running velocity and in contrast with the experimental facts in order to validate the technique. Their results had proven that a transient CFD simulation the use of a two-dimensional computational model can precisely predict VAWT running velocity inside 12% error, with the caution that intermediate turbine overall performance was not precisely captured. **Zhu et al. [52]** aimed at numerically providing a systematic synthesis on the self-starting aerodynamic characteristics of VAWT. They presented the physical model of VAWT and its parameter definitions. Then, they developed the interaction model between the VAWT and fluid by using weak coupling approach; then compared the numerical data of that model with the wind tunnel experimental data to show its feasibility. Moreover, they systematically analyzed the effects of solidity and fixed pitch angle on the self-starting aerodynamic characteristics of the VAWT. Finally, they obtained the quantification effects of the solidity and fixed pitch angle on the self-starting performance of the turbine. Their analysis provided straightforward physical insight into the VAWT self-starting aerodynamic characteristics. **Worasinchai et al. [53]** aimed at checking out the impact of turbine starting capability on standard energy-production capacity. They investigated the development and validation of MATLAB/Simulink fashions of turbines. They investigated the results of load types, specifically resistive heating, battery charging, and grid connection. They mentioned that fundamental contributors to multiplied starting overall performance were aerodynamic improvements, reduction of inertia and changing the pitch

angle of the blades, which were attained from an exploitation of a “mixed-airfoil” blade. The beginning capability had a direct impact on the length that the turbine was operated and consequently its standard power output. The usual behavior of the wind turbine system relied upon on the load type, these impose different torque traits for the turbine to overcome and lead to unique strength manufacturing characteristics. When they used a “mixed-airfoil” blade, the annual energy production of the wind systems increased with the exception of resistive heating loads. Net adjustments in annual energy production were range of 4% to 40% depending on the considered load types and websites. They suggested that the beginning performance and load types had to be considered together in the diagram process. **Zhu et al. [54]** dealt with an investigation of the self-starting aerodynamic characteristics of VAWT under fluctuating wind as the rotational speed of the turbine is not fixed. They developed a weak coupling method to simulate the dynamic interaction between the fluctuating wind and passive rotation turbine. Their results showed that the self-starting aerodynamic characteristics of VAWT would be enhanced if the fluctuating wind with appropriate fluctuation amplitude and frequency. They also found that compared with the fluctuation amplitude, the fluctuation frequency of the variation in wind velocity was shown to have a minor effect on the performance of the turbine. **Worasinchai [55]** evaluated potential benefits obtained from the improvement of starting behavior for both horizontal- and vertical-axis. They presented aerofoil performance characteristics for both steady and unsteady flow needed for the analysis. They conducted all their investigations using a new set of aerodynamic performance data of six aerofoils (NACA0012, SG6043, SD7062, DU06-W-200, S1223, and S1223B). They obtained their data at low Reynolds number (from $6.5x10^4$ to $1.5x10^5$), high angle of attack (through 360°) and high reduced frequency (from 0.05 to 0.20). In order to obtain accurate aerodynamic data at high incidences, they undertook a series of CFD simulations to illustrate effects of wall proximity and to determine test section sizes that offer minimum proximity effects. They made investigations to H-Darriues turbine self-starting capability through the analogy between the aerofoil in Darrieus motion and flapping-wing flow mechanisms. Their investigations revealed that the unsteadiness associated with the predicted and the accurate starting behavior of the rotor could be made when they correctly modelled the transient airfoil behavior. Their analogy investigations indicated that the unsteadiness could be exploited to promote the turbine ability to self-start.

Since Savonius wind turbine is known by its self-starting ability at a low wind speed while Darrieus characterized by its high efficiency. They have to be combined in one hybrid system. A hybrid turbine consists of two turbines on the same shaft. Such a design exploits good features of the two turbines. **Bhuyan and Biswas [56]** designed a VAWT rotor that possesses both self-starting and high-power coefficient simultaneously. They investigated a three bladed H-rotor with unsymmetrical cambered S818 airfoil blades, which showed self-starting characteristics at many of the azimuthal angles. To make the rotor completely self-starting, they incorporated their turbine in a hybrid system with Savonius rotor as its starter. They found that the hybrid design fully exhibited self-starting capability at all azimuthal positions, signified by the positive static torque coefficient values. To improve power performance, the authors investigated the rotor at different Reynolds numbers (Re) between 1.44 $x10^5$ and 2.31 x 10^5 and for five different overlap conditions in the Savonius rotor part. Out of all the designs investigated, the maximum Cp of 0.34 was obtained for the hybrid rotor at Tip Speed Ratio (TSR) of 2.29 and Re of 1.92 x 10^5 for the optimum 0.15 overlap. The optimum hybrid H-Savonius rotor demonstrated better power performance as compared to many of the existing VAWT rotors. **Hosseini and Goudarzi [57]** numerically designed, simulated and evaluated the performance of an innovative hybrid VAWT to obtain an extended operational range and enhance self-starting capabilities using Ansys. A hybrid VAWT consisting of a two-blade modified Savonius Bach-type rotor and a three-blade Darrieus turbine was modeled and analyzed in Computational Fluid Dynamics (CFD) to calculate the characteristic parameters of the rotor system. Results indicated that while the Darrieus turbine had the highest coefficient of power Cp of 48.4% at a TSR of 2.5, it suffered from high start-up torque requirements. The hybrid turbine demonstrated self-starting capabilities while reaching a maximum Cp of 41.4% at a TSR of 2.5 and operation up to a TSR value of 4.5. They declared that their configuration demonstrated improvements to the efficiency and operational range. **El-Nenaey et al. [58]** aimed at numerically combining the favor characteristics of Savonius and Darrieus turbine by producing a hybrid VAWT and evaluated its performance. They built up a numerical model using ANSYS Fluent 17.1 software to simulate the flow over the wind turbine blades. The model was based on three-dimensional, incompressible and unsteady assumptions. They validated their numerical model and used it to evaluate the performance of the hybrid turbine. They compared three different configurations of Savonius, Darrieus and combination of them (hybrid turbine). Their results showed that hybrid vertical axis turbine which its Savonius rotor is located inside Darrieus rotor achieved higher starting torque. Besides at high Tip Speed Ratio (TSR) the hybrid took the advantage of its drag type blades as a guide for the flow to Darrieus

blades. **Hammond et al. [59]** aimed at designing a VAWT for urban use. They analyzed behavior of the wind in that urban location. They evaluated different turbine types and determined that a new type of turbine should be created to be incorporated both lift and drag. For their turbine, an airfoil would be necessary along with a shroud for protecting and increasing wind velocities. Then their overall design was created, manufactured, tested and achieved a good performance. **Mohammed et al. [60]** intended to design, fabricate and experimentally investigated the performance of hybrid VAWT on residential buildings. A building model with gable rooftop was design and fabricated for use in testing of the hybrid VAWT. Their results showed that the hybrid VAWT mounted on the building rooftop yield up to 63% more energy compared to the bare-hybrid VAWT (without building). They observed similar improvement in performance of the hybrid VAWT in the rotational speed, mechanical power and the coefficient of torque. Thus their results indicated that urban buildings are suitable for the mounting of the hybrid VAWT. **Pallotta et al. [61]** experimentally described a novel hybrid Savonius-Darrieus combined rotor. They aimed optimizing performances in medium-low wind regimes, by using a careful design of the shape, size and relative positions of Savonius and Darrieus blades. Their scaled turbine model was tested in wind tunnel to derive instantaneous and averaged velocity fields by means of Particle Image Velocimetry (PIV) to view wakes and specific fluid flow phenomena on each single configuration (Savonius or Darrieus) and interactions on the combined geometry. Their results were coupled with electrical measurements to determine global performances, efficiency and best working conditions for each separate turbine and for the combined turbine. Data were also compared with results obtained by other authors in previously reported combined hybrid configurations. Their proposed system was able to work with good performances (power coefficient equal or slightly lower than 0.2 and for tip speed ratios between 0.5 and 4). **Alam and Iqbal [62]** presented the design of a hybrid turbine based on a straight bladed Darrieus (lift type) turbine along with a double step Savonius (drag type) turbine. Four-blade Darrieus rotor was placed on top of a Savonius rotor. Their hybrid vertical axis turbine had much better self-starting characteristics and better conversion efficiency at higher flow speeds. Their hybrid turbine was built and tested in variable speed water currents. It could also be used as a wind turbine. They mentioned that it would be used to generate power at the sea floor for an instrumentation system.

Still Darrieus turbine has its self-starting problem and as a solution it may be combined in Double-Darrieus hybrid system to be self-starting and to have a high power coefficient. **Ahmad et al. [63]** emphasized designing a straight-bladed Double-Darrieus hybrid VAWT. They performed Computational Fluid Dynamics (CFD) analysis using the sliding and dynamic meshing techniques and employed various datasets in the design of experiments to determine optimal configurations. They established a quadratic equation based on a regression model and applied response surface methodology to determine the accuracy of the model by analysis of variance, goodness of fit, investigation of residuals, and R-squared values. Moreover, they obtained the optimized chord length, number of blades, pitch angle, distance of blades from the central rotating shaft, and rotor height to be 0.547 m, 03, -3.41º, 0.789 m and 1.605 m, respectively. For comparison, they analyzed a standard H-rotor Darrieus configuration, comprising symmetric airfoils and existing Darrieus-Savonius hybrid VAWTs. The positive static torque coefficient at all azimuth angles indicates that the proposed hybrid wind turbine was completely self-starting. The self-starting speeds of standard Darrieus and the proposed hybrid wind turbine were at a wind speed of 3.65 m/s and 2.81 m/s, respectively. Their proposed approach enabled the determination of the optimum design configuration of a hybrid Vertical Axis Wind Turbine, along with a high-fidelity analysis in the early design phase. To improve the self-starting characteristics and to enhance the low wind speed performance, **Kumar et al. [64]** proposed a Dual rotor Darrieus Turbine (DD) with secondary rotor in addition to the primary rotor. They evaluated experimentally the proposed rotor with two set of blades as a possible means of achieving higher static torque and thus promoting self-starting capability. Although, the design parameters for the secondary rotor had such as solidity, appropriate airfoil, secondary rotor diameter, secondary rotor offset with respect to primary rotor required extensive optimization. Power, dynamic and static torque coefficients were obtained through wind tunnel test and compared with Conventional Darrieus (CD) turbine (only with primary rotor). Their results indicated that the novel dual rotor had improved the self-starting capability at the reduced power performance.

therefore in this thesis explore various parallel configuration instead of offset configuration to study the differences between them.

CHAPTER THREE

Experimental Model And Numerical Model

3.1 EXPERIMENTAL MODEL

3.1.1 Introduction

The Experimental chapter encompasses a comprehensive examination of the experimental setup and procedures employed in the study. Subsequently, the chapter discusses the various components and instrumentation utilized in the experimental setup, highlighting their role in capturing accurate data. This includes the selection and calibration of measuring instruments. The section further explores specific measuring techniques, such as wind speed measurement techniques. Additionally, load cells and force measurement techniques are examined. The inclusion of encoders and rotational speed measurement techniques is also addressed to enable accurate measurement of the turbine's rotational performance. Moreover, the integration of Arduino, a versatile microcontroller platform, is discussed in relation to its utility in data acquisition and control systems.

Moving on, the chapter transitions to the exploration of wind tunnel testing, beginning with an introduction to its significance and applications in the field of wind turbine engineering.

Furthermore, the chapter covers the calculations involved in experimental studies, emphasizing the importance of data processing and analysis. Figure 3.1 shows The Experimental Vertical Axis Wind Turbine (VAWT) in Wind Tunnel used in this study.

Figure 3.1: Experimental Vertical Axis Wind Turbine (VAWT) in Wind Tunnel.

3.1.2 Experimental Setup

3.1.2.1 Construction of Experimental Setup

The experiment conducted in this study involved a structural test bench that accommodated a Darrieus wind rotor, various measurement devices, and a wind tunnel. The wind turbine was positioned at the center of the inlet section for the wind tunnel, with dimensions of 30 cm × 30 cm × 100 cm. To minimize friction torque and ensure accurate measurements, the Darrieus rotor shaft was supported by two low-friction bearings arranged in a cantilever configuration. The design allowed for easy replacement of different rotor types during the experimentation process through the use of bolts and nuts. Figure 3.2 shows inlet section for wind tunnel.

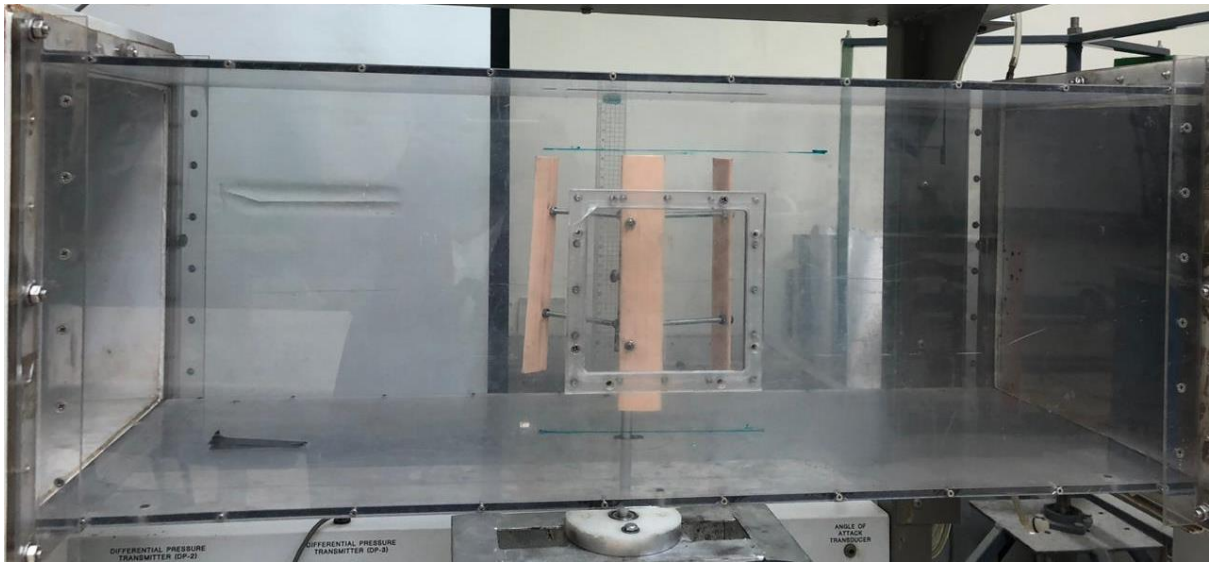

Figure 3.2: Experimental VAWT in inlet Test Section in Wind Tunnel

Wind velocity was determined using. 1. pitot static tube connected to a manometer. To load the Darrieus rotor, 2.a brake drum dynamometer, acting as a pulley, was employed. 3. A two load cell was connected via a 2 mm diameter fishing nylon wire. It should be noted that friction can significantly impact torque measurements in the rotating Darrieus rotor, particularly in the bearings and the nylon wire wound around the rotor shaft. To minimize friction, the bearing seals were removed, and the bearings underwent thorough cleaning with petrol to eliminate grease before installation.

During the experiments, the wind velocity was adjusted to correspond to a specific Reynolds number, and the rotor was allowed to rotate from a no-load speed. the bearings were sprayed with a commercially available lubricant for optimal performance.

The experimental procedure involved several steps. Firstly, the wind tunnel fan was operated at a specified velocity. Torque and RPM values were initially recorded at T = 0 and subsequently at incremental torque increments until the turbine came to a stop. Readings were taken separately for each speed. In the Double blade case, the inner blade was inserted at the closest point to the rotor, and readings were recorded accordingly. The distance of the inner blade was incrementally changed from 1 cm to 7 cm, and the above steps were repeated for each 1 cm change.

Finally, the recorded data was acquired through an Arduino and processed using specific software programs tailored for data analysis and interpretation. Figure 3.3 shows Experimental Vertical Axis Wind Turbine (VAWT) in Inlet Section of Wind Tunnel with Measuring Instruments Enclosure

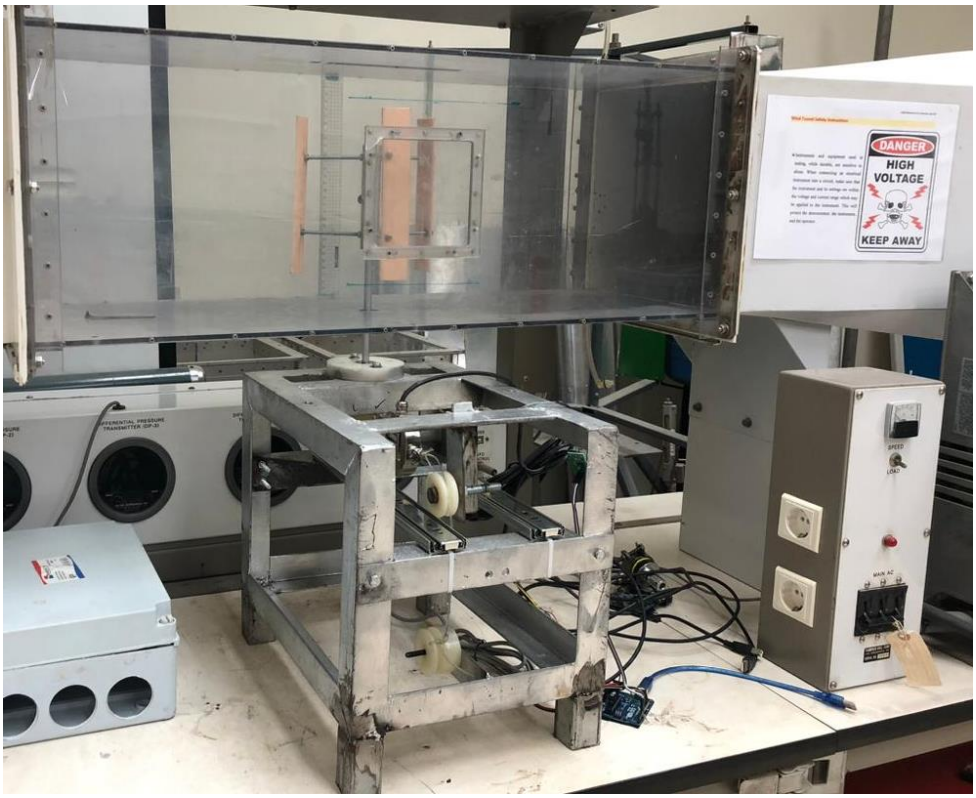

Figure 3.3: Experimental Vertical Axis Wind Turbine (VAWT) in Inlet Section of Wind Tunnel with Measuring Instruments Enclosure

- Wind turbine Geometrical and Experimental parameters

Experimental parameters For Single blade configuration shown in Table 3.1.*Table*

Table 3.1: Geometrical and Experimental Parameters for Single Blade Configuration.

Parameters	Experimental
Number of blades N	3
Blade Hight	20 cm
Blade Profile	NACA0018
VAWT Radius R	10 cm
Chord length c	3.5 cm
Solidity σ	1.05

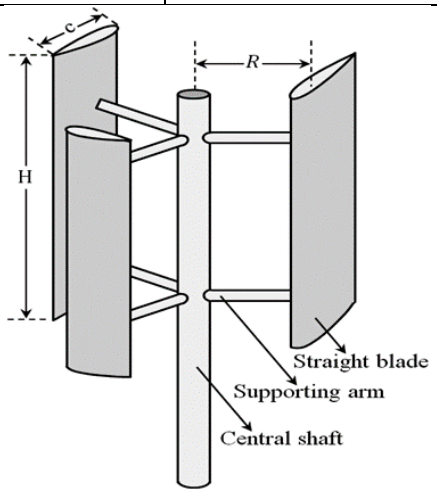

Figure 3.4: Straight-Bladed Vertical Axis Wind Turbine

Experimental parameters For Double blade configuration shown in Table 3.2

Table 3.2: Geometrical and Experimental Parameters for Double Blade Configuration.

Parameters	Experimental
VAWT Diameter D	20 cm
Number of outer blades N	3
Number of inner blades N	3
Outer Blade Hight	20 cm
Inner Blade Hight	10 cm
Blade Profile	NACA0018

Air speeds in the wind tunnel are comparative to average range of wind speeds in Egypt from wind atlas by employing Reynolds number formula as part of the similarity

which is based in equations from 1 to 4. Actual air velocity is calculated to be from 2.3 to

4.4 m/s

$$Re_{model} = Re_{actual} \quad (3.1)$$

$$\frac{\rho v d}{\mu}_{model} = \frac{\rho v d}{\mu}_{actual} \quad (3.2)$$

$$v_m d_m = v_a d_a \quad (3.3)$$

$$v_m = v_a \frac{d_a}{d_m} \quad (3.4)$$

$$v_a = 0.1 * v_m \quad (3.5)$$

Power and power coefficient can be calculated:

$$p = T * \omega \quad (3.6)$$

$$C_p = \frac{P}{0.5 * \rho * V^3 * A} \quad (3.7)$$

- Manufacturing of Blades for the Wind Turbine

To manufacture the blades, the dimensions and design were translated into a SolidWorks drawing. The chosen material for the blades is a 3D printing photopolymer resin series, which offers suitable properties for the application.

After cutting and finishing the blades, additional modifications were made to ensure the successful completion of the project. Two holes were created in each blade and corresponding holes were made through the shaft. These holes allow for the insertion of bolts and nuts, which secure the blades firmly onto the shaft, ensuring proper attachment and functionality. Experimental Model of a Single and Double Vertical Axis Wind Turbine shown in Figure 3.5 and Figure 3.6.

Figure 3.5: Experimental Model of a Single Vertical Axis Wind Turbine.

Figure 3.6: Experimental Model of a double Vertical Axis Wind Turbine.

3.1.2.2 Measuring Instruments

- Selection and Calibration of Measuring Instruments

In order to ensure the validity and accuracy of the experimental results, a careful selection and calibration process was conducted for the measuring instruments utilized in the study. The

measuring instruments employed in the experimental setup included the Weight Sensor (Load Cell), Weight Sensor (SS Beam Load Cell), Rotary Incremental Encoder, and Arduino.

The selection of appropriate measuring instruments was based on their suitability for capturing the desired parameters and their compatibility with the experimental requirements. Load Cells and Force Measurement Techniques

- Weight Sensor (Load Cell) 0-1000g

The load cell may be used to measure the force F1 on tight side of the nylon wire in kg.

Weight Sensor (Load Cell) 0-1000g shown in Table 3.3.

Table 3.3: Weight Sensor (Load Cell).

Specifications	Range
Rated load	1000g
Output	± 0.05mv / v
Temperature zero drift	0.1% F.S
Output sensitivity	1.0 ± 0.1 mv / v

- Weight Sensor (SS Beam Load Cell 50Kgf-10tf) (SS300)

The load cell is used to measure the force F2 on the other side of the nylon string in kg.

Weight Sensor SS Beam Load Cell shown in Table 3.4.

Table 3.4: Weight Sensor SS Beam Load Cell.

Parameter	**Unit**	**Range**
Rated output (R.O)	Mv/v	2.0.030±0.005
Zero balance	Mv/v	0±0.02
Combined error	%	0.03
Repeatability	%	0.01

- Encoder and rotational speed

The Rotary incremental Encoder (200 PPR - 5:24V) YT06-OP with 200 pulses per revolution (PPR) is a quadrature incremental encoder utilized for measuring the rotation of a shaft.

. Rotary incremental Encoder shown in Table 3.5.

Table 3.5: Rotary Incremental Encoder.

Parameters	Range
Resolution	200 Pulse/Rotation
Encoding Method	Incremental
Input Voltage	5 - 24VDC
Maximum Rotating Speed	6000rpm

- Arduino

The Arduino Uno R3 (Latest Revision) - Clone is a microcontroller board based on the ATmega328P.

3.1.2.3 Calculations in Experimental Studies

1. Operate the wind tunnel fan at a specified velocity.
2. The torque and RPM values were recorded initially at T = 0, and then at increments of torque until the turbine came to a stop.
3. Readings were taken at each speed separately.
4. The inner blade was inserted at the closest point to the rotor, and readings were taken accordingly.
5. The distance of the inner blade was incrementally changed from 1 cm to 7 cm, and the steps 1, 2, and 3 were repeated for each change of 1 cm.

After the Experimental measurements are carried out, the following parameter can be calculated

$$TSR = \frac{\omega \times R}{v} \quad (3.8)$$

$$\omega = \frac{2 \times \pi \times N}{60} \quad (3.9)$$

3.2 Numerical Model

3.2.1 Introduction to numerical simulation

This section provides an overview of the purpose and significance of numerical simulation using Ansys Fluent for studying single blade and double blade vertical axis wind turbines (VAWTs). The focus of this study is to investigate three-bladed Darrieus vertical axis wind turbine (VAWT) using computational fluid dynamics (CFD) modeling. The primary objective of this phase was to analyze the VAWT's aerodynamic performance under varying wind speeds. The simulation domain employed in this study is similar to the experimental setup, allowing for direct comparison between wind tunnel measurements, numerical simulations, and their respective results.

3.2.2 Overview of the turbine and data

The turbine used in the experiment has the following properties, The CFD model was developed based on the principles of the Reynolds-averaged Navier-Stokes equations (RANS) to simulate the fluid flow around the VAWT. The geometry of the wind turbine, including the airfoil profile, chord length, number of blades, radius, height, and length, was accurately represented in the numerical model. The chosen airfoil for the blades was the NACA 0018, with a chord length (c) of 0.035 m. The wind turbine featured three blades (N = 3), with a radius (R) of 0.1 m, a height (h) of 0.2 m, and a length (L) of 1 m, the wind turbine in the experimental setup exhibited varying rotational speeds, Numerical model main geometrical features and operational parameters showed in Table 3.6.

Table 3.6: Overview of The Dimensions of The VAWT Used In The Experiment.

Parameters	Experimental
VAWT Diameter D	20 cm
Number of blades N	3
Blade Hight	20 cm
Blade Profile	NACA0018
VAWT Radius R	10 cm
Chord length c	35 cm
Solidity σ	1.05

The first step is the optimization process is generating the geometry. The 2D model, Blades of VAWT have been created using Solidworks and ANSYS. This geometry is described as

parameter in Table 3.6. And Some important dimensions are indicated in the Figure 3.7 For the purpose of numerical analysis, Computational Fluid Dynamics (CFD) code FLUENT 2-D is used and seven different models are numerically examined at the different wind speed and compared among them.

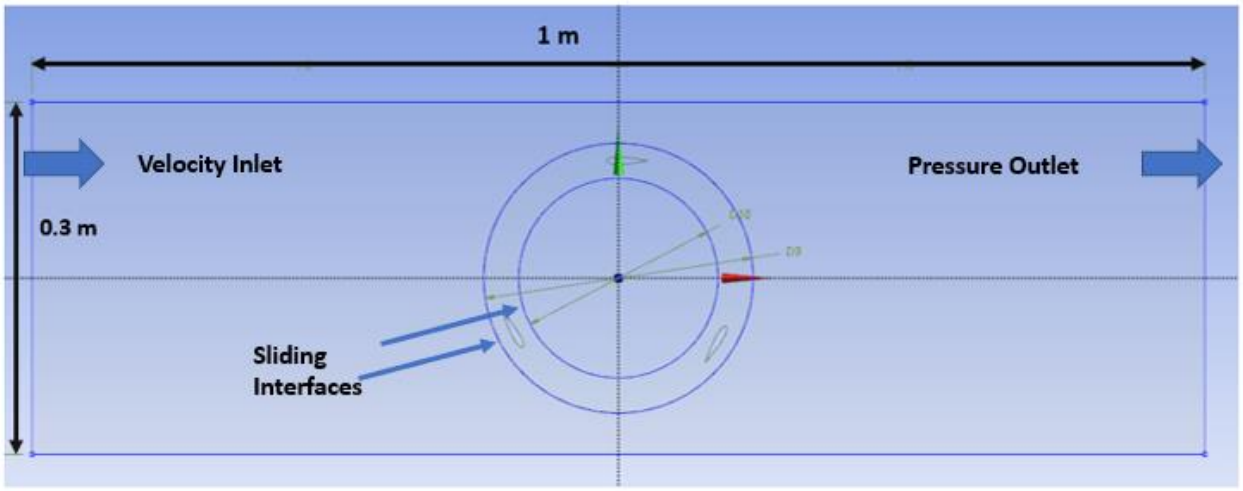

Figure 3.7: 2D Model of The Vertical Axis Wind Turbine

The blade profile for the wind turbine was selected based on the aforementioned advantages of the NACA 0018 airfoil. Its higher lift-to-drag ratio, reduced drag, favorable stall characteristics, versatility, historical success, and performance at low wind speeds made it an ideal choice for optimizing the turbine's performance and efficiency. the selected blade profile is showed in Figure 3-8.

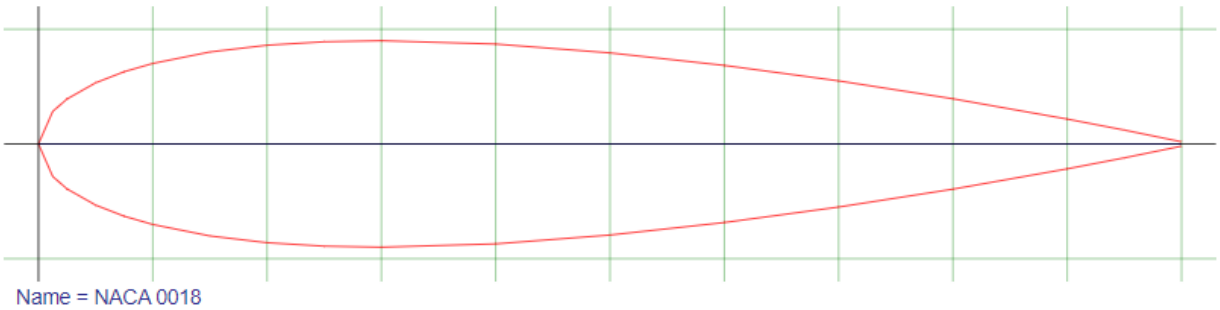

Figure 3.8: NACA 0018 Airfoil

Blade Profiles, The NACA 0018 airfoil is advantageous for Darrieus Vertical Axis Wind Turbines (VAWTs) due to several factors, Enhanced lift-to-drag ratio: The curved shape of the NACA 0018 airfoil allows it to generate increased lift while minimizing drag. This

characteristic significantly improves the turbine's aerodynamic efficiency and enhances its power generation capabilities.

Reduced drag: The streamlined design of the NACA 0018 airfoil contributes to a decrease in drag, enabling smoother and more efficient rotation of the turbine blades in the wind. This reduction in resistance enhances the overall performance of the turbine.

Favorable stall characteristics: The NACA 0018 airfoil exhibits favorable stall characteristics, meaning it is less prone to experiencing flow separation and loss of lift at high angles of attack. This attribute ensures the turbine's effective operation even in turbulent wind conditions.

Versatility and applicability: Extensive study, testing, and documentation have been conducted on the NACA 0018 airfoil. Its performance characteristics have been thoroughly analyzed and optimized, establishing it as a reliable choice for Darrieus VAWTs.

Historical usage and success: The NACA 0018 airfoil have a long-standing history of successful implementation in vertical axis wind turbines, particularly in Darrieus designs. Its efficient and reliable performance has been proven, making it a preferred choice for turbine designers and manufacturers.

Additionally, the NACA 0018 airfoil is particularly well-suited for small-scale wind turbines and demonstrates excellent performance at low wind speeds. This quality further enhances its appeal for applications that require efficient extraction of energy from low-velocity wind resources.

In conclusion, the NACA 0018 airfoil's superior lift-to-drag ratio, reduced drag, favorable stall characteristics, versatility, historical success, and commendable performance at low wind speeds make it an ideal choice for improving the performance and efficiency of Darrieus Vertical Axis Wind Turbines. [72]

3.2.3 Meshing

In this study, simplified extrusion models were employed, leading to the utilization of a 2-D simulation methodology. To facilitate the simulation process, the CFD ANSYS solver was employed to generate the required mesh.

To ensure accurate representation of the flow dynamics near the blade and the critical interface, a highly refined orthogonal grid was implemented. Notably, particular emphasis was placed on the region encompassing the inlet of air towards the rotor area, as well as on achieving a smooth

transition downstream. It is worth mentioning that all the generated meshes incorporated three blades in their configurations, ensuring consistency throughout the analysis, Mesh and Interface shown in Figure 3.9, Figure 3.10 and Figure 3.11.

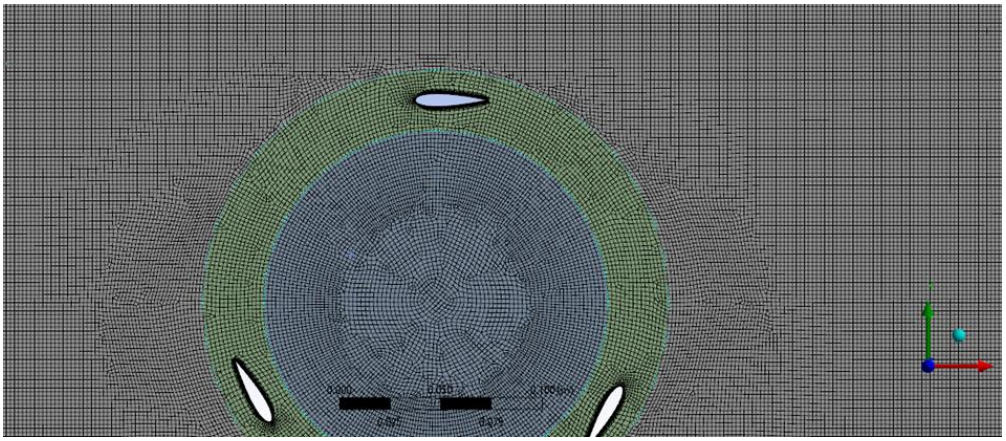

Figure 3.9: A View of Final Mesh Used

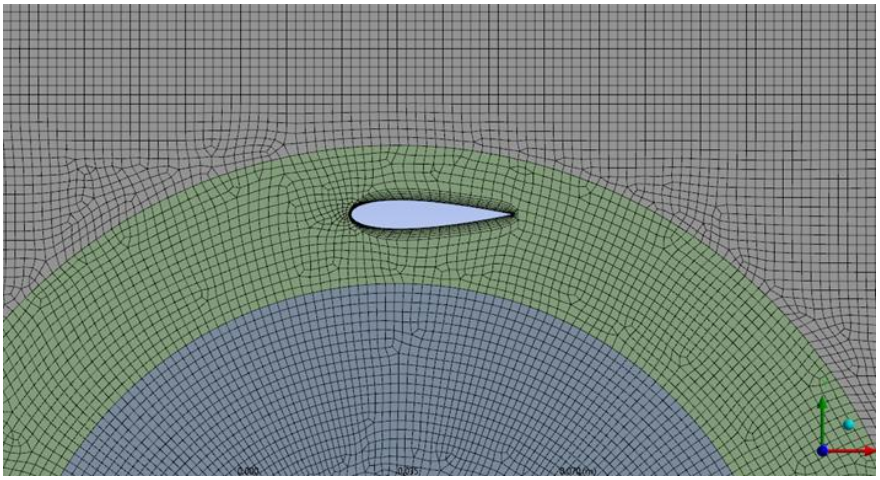

Figure 3.10: Mesh and Interface View

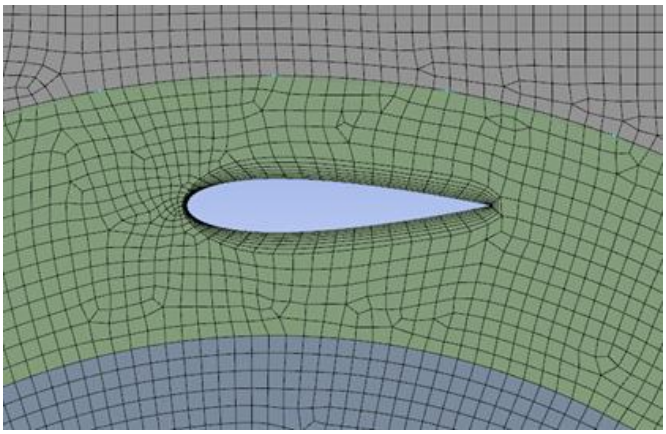

Figure 3.11: Mesh With Inflation.

- Grid Independence Study and Mesh Characteristics

An unstructured mesh composed of quadrilateral elements was generated to adequately resolve the boundary layer surrounding the airfoil. A mesh independency study was carried out. Figure 3.11 shows the relation between lift coefficient and the number of elements at an air velocity of 23 m/s. For element numbers of 7.7×10^4. Mesh view near turbine blades are shown in Figure 3.12.

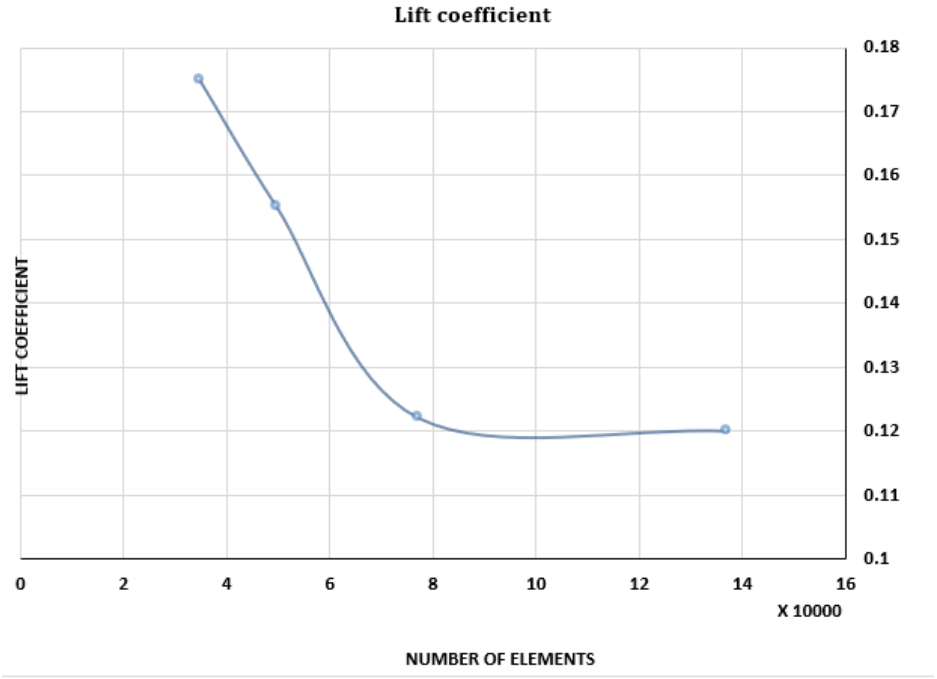

Figure 3.12: Relation Between Lift Coefficient and Number of Elements at Air Velocity of 23 m/s.

Table:3.7 Relation Between Lift Coefficient and Number of Elements

Number of Element	34647	49691	77258	137092
Lift coefficient	0.175	0.155	0.122	0.12
Inflation option	Smooth transition	Smooth transition	Smooth transition	Smooth transition

3.2.4 Solver settings

Several configurations needed to be modified to enable the execution of simulations. This section provides a concise summary of the settings utilized in FLUENT, offering relevant details when necessary. The structure of this section adheres to the layout of FLUENT itself, specifically the layout of the ANSYS 2023R1 edition of FLUENT.

- General Solution Setup

In this context, The settings are configured for a two-dimensional (2D) simulation .

- Models

In this study, the k-omega (2 equation) shear stress transport (SST) turbulence model was employed. This model was chosen to accurately capture the effects of viscosity and turbulence on the flow behavior within the computational domain.

- Materials

the ANSYS FLUENT software employed the standard air properties for the airflow and solid aluminum properties. The selected air composition was representative of typical atmospheric conditions and served as the basis for the simulation. The standard air in ANSYS FLUENT was characterized by a density (ρ) value of 1.225 kg/m³ and a dynamic viscosity (μ) of 1.7894×10^{-5} kg/(m·s).

- Cell Zone Conditions

The sub-menu of cell zone conditions provides a comprehensive list of distinct zones present within the mesh. In the current study, the mesh comprises three zones, namely the outer and inner fluid zones, the surrounding subzone, and the annulus housing the turbine blades. The arrangement of these zones is depicted in the accompanying figure

To effectively simulate the rotational motion of the turbine, a specific approach known as the sliding mesh method is employed. In this method, the mesh within the blade fluid zone undergoes rotation around the turbine's center with a consistent angular velocity denoted as $\omega = 20.9$ rad/sec. Notably, the angular velocity is adjusted for each case run to explore different velocities and their corresponding effects.

Presented in the results obtained from various ANSYS cases, each characterized by different angular velocities and corresponding velocities. The angular velocities are calculated using equation (8) according to wind speed.

$$v = \omega r \quad (8)$$

This table serves to provide a comprehensive overview of the relationship between angular velocity and velocity within the simulated system. Velocity and Angular Velocity Combinations in ANSYS Cases presented in Table 3.8.

Table 3.8: Velocity and Angular Velocity Combinations in ANSYS Cases.

Case	Velocity (v (m/s))	Angular Velocity (ω (rad/s))
1	23	20.9
2	26	48.1
3	30	47.1
4	33	39.7
5	37	50.8
6	40	48.1
7	44	50.2

- Boundary Conditions

The boundary conditions are, The inlet velocity, set at 23 m/s, outer zone , turbine walls , wind tunnel walls and middle zone from the front, the interface between the outer zone and middle zone .

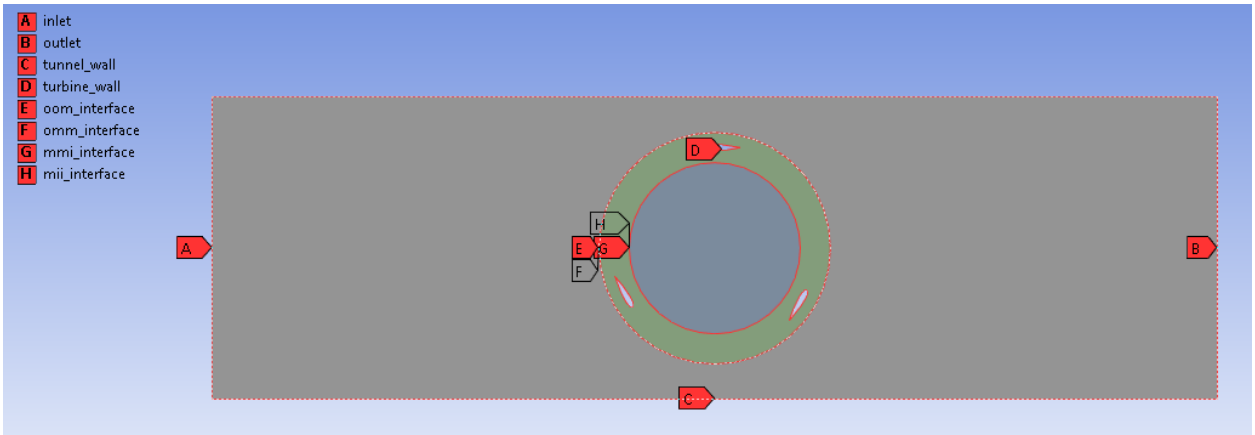

Figure 3.13: Boundary Condition

Additionally, the tunnel wall is considered a stationary wall with no-slip characteristics, while the turbine wall is modeled as a moving wall. The rotational speed of the turbine wall corresponds to the angular velocity specified in Table 3.7, ensuring consistency between the speed of the wall and the associated cell zone.

In the case of a 2D simulation, this assumption allows for the determination of other relevant parameters Reference Value, such as the area (A), which is calculated as 0.04 m^2. Additionally, the depth is set to 0.2 m, the length is specified as 0.2 m, and the velocity and air properties are

assigned values consistent with the previously described boundary conditions and material properties.

By accurately configuring the values within this sub-menu, FLUENT is able to correctly calculate the coefficient of the moment (Cm) and power coefficient (CP) and incorporate it into the overall analysis.

- Solution Initialization

The simulation employed the Hybrid initialization method for solution initialization.

- Calculation Settings

To determine an appropriate time step size, considerations such as the rotational speed of the system are considered. For example, considering a rotational speed of 450 revolutions per minute (rpm), the corresponding time period (T) can be calculated as 7.6 cycles. The time step (delta T) is obtained as the reciprocal of the number of cycles, resulting in a value of 0.13. To further refine the temporal resolution, the time step for one degree (Delta T) can be calculated by dividing the time step by 360, resulting in a value of 0.00036. Finally, to achieve even finer granularity, the time step for half a degree (Delta T) is determined by dividing the time step for one degree by 2, yielding a value of 0.00018, different time step showed in Table 3.9.

Table 3.9: different delta T with time step

W	delta T	t-s
20.9	0.3	0.0004
48.1	0.13	0.0001
47.1	0.133	0.0001
39.7	0.158	0.0002
50.8	0.123	0.0001
48.1	0.13	0.0001
50.24	0.125	0.0001

- **The Shear-Stress Transport (SST k-ω) model**

The SST k-ω turbulence model is a two-equation eddy-viscosity model. The SST formulation combines the best of two models. The use of a k-ω formulation in the inner parts of the boundary layer makes the model directly usable all the way down to the wall through

the viscous sub-layer, hence the SST k-ω model can be used as a Low-Re turbulence model without any extra damping functions. The SST formulation also switches to a k-ε behaviour in the free-stream and thereby avoids the common k-ω problem that the model is too sensitive to the inlet free-stream turbulence properties. Also, SST k-ω model has a good behaviour in adverse pressure gradients and separating flow. The transport equations for SST k-ω model are

Turbulence kinetic energy equation

$$\frac{\partial k}{\partial t}+\overline{u}_j\frac{\partial k}{\partial x_j}=P_k-\beta^* k\omega+\frac{\partial}{\partial x_j}\left[\left(\upsilon+\sigma_k\upsilon_T\right)\frac{\partial k}{\partial x_j}\right] \tag{3.10}$$

Specific dissipation rate equation

$$\frac{\partial \omega}{\partial t}+\overline{u}_j\frac{\partial \omega}{\partial x_j}=\alpha S^2-\beta\omega^2+\frac{\partial}{\partial x_j}\left[\left(\upsilon+\sigma_w\upsilon_T\right)\frac{\partial \omega}{\partial x_j}\right]+2\left(1-F_1\right)\sigma_{w2}\frac{1}{\omega}\frac{\partial k}{\partial x_i}\frac{\partial \omega}{\partial x_i} \tag{3.11}$$

Kinematic eddy viscosity equation $\upsilon_T=\dfrac{\alpha_1 k}{\max\left(\alpha_1\omega, SF_2\right)}$ (3.12)

The closure coefficients and auxiliary relations are:

$$F_2=\tanh\left\{\left[\max\left(\frac{2\sqrt{k}}{\beta^*\omega y},\frac{500\upsilon}{y^2\omega}\right)\right]^2\right\},\ P_k=\min\left(\tau_{ij}\frac{\partial \overline{u_i}}{\partial x_j},10\beta^* k\omega\right), \tag{3.13}$$

$$F_1=\tanh\left\{\left\{\min\left[\max\left(\frac{\sqrt{k}}{\beta^*\omega y},\frac{500\upsilon}{y^2\omega}\right),\frac{4\sigma_{w2}k}{CD_{kw}y^2}\right]\right\}^4\right\} \tag{3.14}$$

$$CD_{kw}=\max\left(2\rho\sigma_{w2}\frac{1}{\omega}\frac{\partial k}{\partial x_i}\frac{\partial \omega}{\partial x_i},\ 10^{-10}\right) \tag{3.15}$$

$\phi=\phi_1F_1+\phi_2\left(1-F_1\right)$ (as $\phi=\alpha\ ,\beta\ ,\sigma_k,\sigma_w,\ \phi_1=\alpha_1,\beta_1,\sigma_{k1},\sigma_{w1}$, and $\phi_2=\ \alpha_2,\beta_2,\sigma_{k2},\sigma_{w2}$)

3.2.5 Summary

The chapter encompasses four key sections that contribute to the overall understanding and implementation of the numerical simulation. These sections include "Introduction to Numerical Simulation," "Overview of the Experimental Turbine and Data," "Meshing," and "Solver Settings."

The first section, Introduction to Numerical Simulation, provides a foundational understanding of the numerical modeling approach employed in the study. It introduces the concept of numerical simulation and its significance in analyzing and predicting the behavior of the turbine system under investigation.

The second section, Overview of the Experimental Turbine and Data, presents a comprehensive overview of the experimental turbine used as the basis for the numerical modeling. It describes the key characteristics and specifications of the turbine, including its geometry, operating conditions, and experimental data obtained from previous studies. This overview serves as a crucial reference for the subsequent numerical modeling efforts.

The third section, Meshing, delves into the process of generating the computational mesh for the numerical simulation. It discusses the methodology and considerations involved in creating a suitable mesh, including grid refinement around critical areas such as the turbine blades and interfaces. This section emphasizes the importance of an accurate and well-structured mesh for obtaining reliable results and highlights the use of three blades in the generated meshes.

The fourth section, Solver Settings, focuses on the configuration and settings of the solver used in the numerical simulation. It covers various aspects such as the choice of solver type, the treatment of boundary conditions, and the selection of solution initialization methods. This section outlines the specific solver settings used in the study and provides insights into their influence on the simulation outcomes.

Collectively, these sections form a comprehensive overview of the numerical modeling approach employed in the study. They establish the foundation for understanding the numerical simulation process, describe the experimental turbine and associated data, explain the meshing procedures, and highlight the solver settings employed. This chapter sets the stage for subsequent analyses and discussions, facilitating a deeper understanding of the numerical model and its application to the turbine system under investigation.

CHAPTER FOUR

RESULTS AND DISCUSSIO

4.1 Results

The chapter begins by focusing on the analysis of the single blade experimental and numerical results, followed by their respective validations. Subsequently, the attention is shifted towards the double blade experimental and numerical results. Finally, a thorough discussion is provided, encompassing a comparative analysis between the single blade and double blade configurations, as well as the examination of additional parameters such as the most efficient position for inlet blade and wind speed velocities.

The presentation of the single blade experimental and numerical results serves as a fundamental basis for evaluating the performance and characteristics of the turbine in an isolated blade configuration. This examination involves the analysis of various parameters, including power output. Furthermore, the experimental results are compared and validated against the corresponding numerical simulations to ensure the accuracy and reliability of the numerical model.

Following the evaluation of the single blade results, the focus shifts towards the double blade experimental and numerical results. This investigation explores the overall turbine performance. The experimental data is meticulously analyzed and compared with the numerical simulations to ascertain the consistency and agreement between the two approaches.

The discussion aims to provide a comprehensive understanding of the experimental and numerical results obtained throughout the study. It offers insights into the effectiveness of the turbine configurations, the accuracy of the numerical simulations, and the impact of various parameters on the turbine's performance. Moreover, it encourages critical thinking and facilitates the identification of areas for further improvement and optimization.

4.1.1 Single Darrieus

This section is dedicated to the discussion of the single blade vertical axis wind turbines configuration.

4.1.1.1 Experimental Results

This section presents the experimental results were performed with different velocities obtained for the single blade Darrieus wind turbines. The blade distance from the rotor was kept at 10 cm for the single blade configuration. The power coefficient (Cp) values obtained from the experiments are summarized in Figure 4.1.

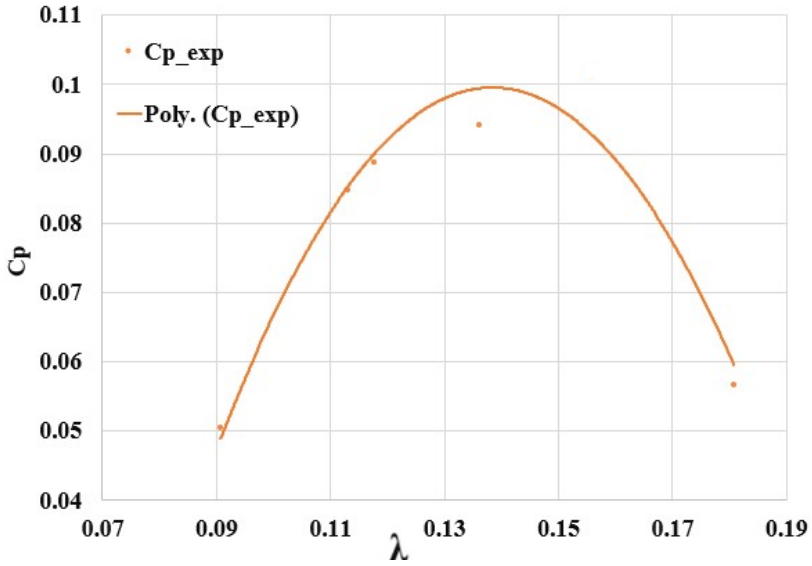

Figure 4.1: Experimental Results for Single Blade (at Distance 10 cm from the rotor).

The experimental results for the single blade configuration show power coefficient values ranging from 0.050447779 to 0.101276102. These results provide empirical data on the performance of the single blade design under different operating conditions.

in the results obtained from the experiments conducted in this thesis, the tip speed ratio within the range of 0.1 to 0.2.

The relation between solidity and airfoil dimensions is in equation (5.1):

$$\sigma = \frac{bc}{R} \qquad (5.1)$$

4.1.1.2 Numerical Results

This section present the simulations results. From the simulations the results were presented and discussed in this section. The numerical simulations were conducted to investigate the aerodynamic behavior and flow characteristics of the Darrieus wind rotor. In this section, we present the results obtained from these simulations.

- **Air flow velocity distributions:**

The simulations allowed for the visualization of air flow velocity distributions around the wind rotor at air velocity of 26 m/s. Contour plots were generated to depict the variations in air flow velocities across the rotor blades and the surrounding regions. These contour plots provided insights into the flow patterns, including regions of higher and lower velocities, as well as the interaction between the blades and the incoming airflow. As illustrated in Figure 4.6.

Figure shows velocity distributions at 26 m/s: θ = 0° and 90°. θ = 0° demonstrated efficient energy use, proper blade alignment and maximized turbine efficiency. While θ = 90° led to

flow separation, hampering energy utilization. θ = 180° also yielded favorable results. θ = 270° had minor impact on power generation and efficiency due to blade's end position. Air flow velocity distributions illustrated in Figure 4.2, 4.3, 4.4, and 4.5.

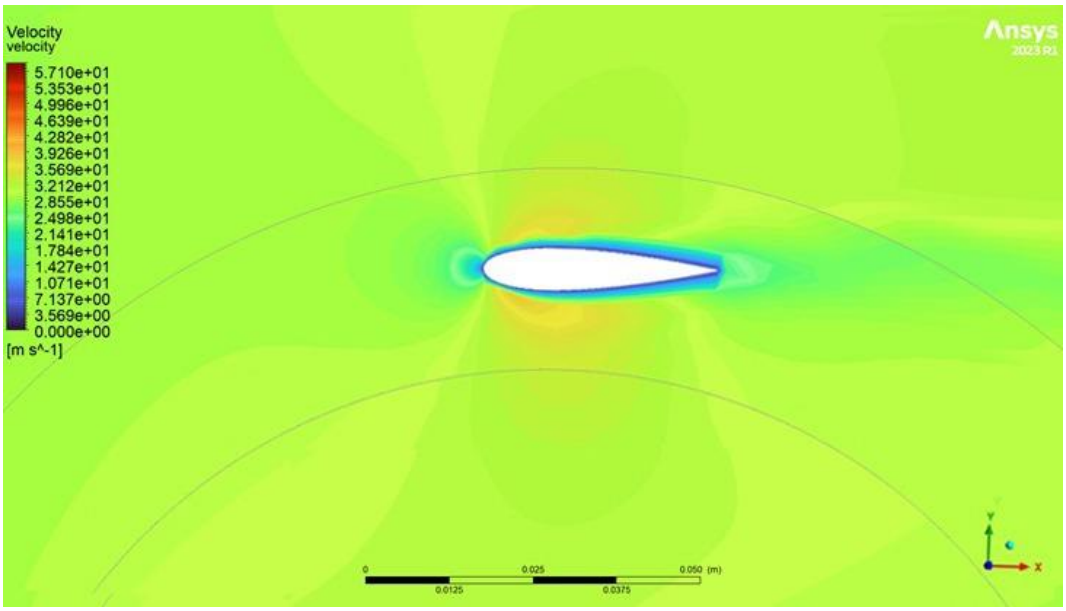

Figure 4.2: Air Flow Velocity Distributions at Air Velocity of 26 m/s, at (a) θ = 0°

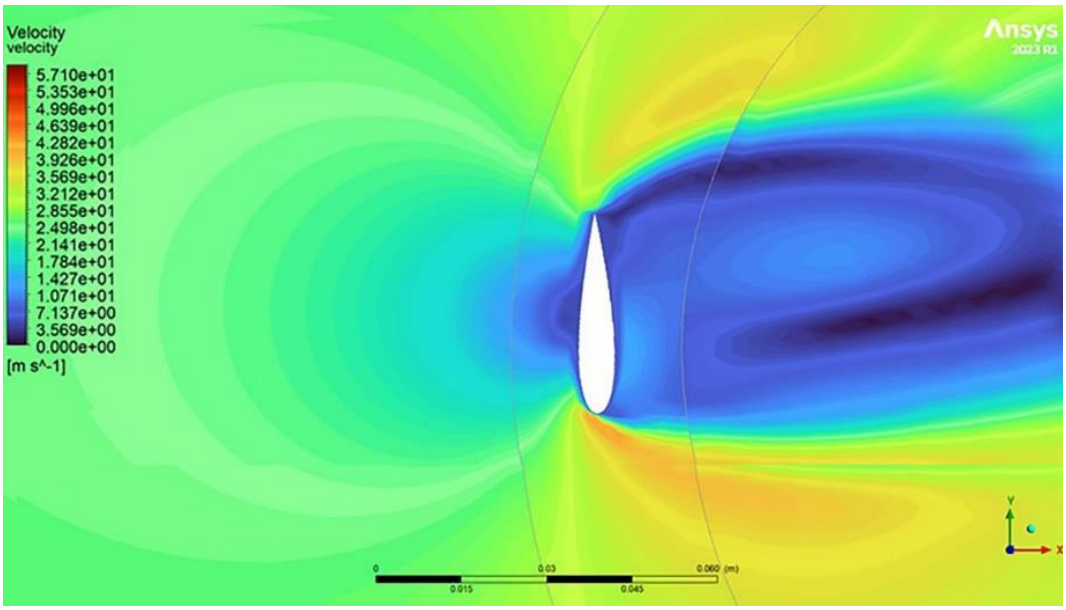

Figure 4.3: Air Flow Velocity Distributions at Air Velocity of 26 m/s, at (a) θ = 90°,

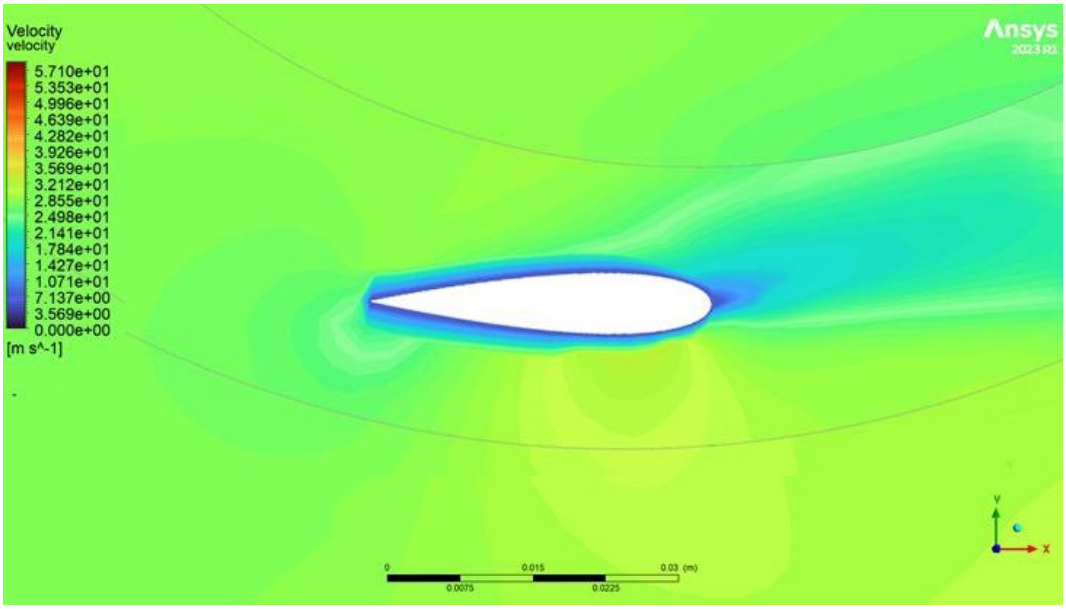

Figure 4.4: Air Flow Velocity Distributions at Air Velocity of 26 m/s, at (a) θ = 180°

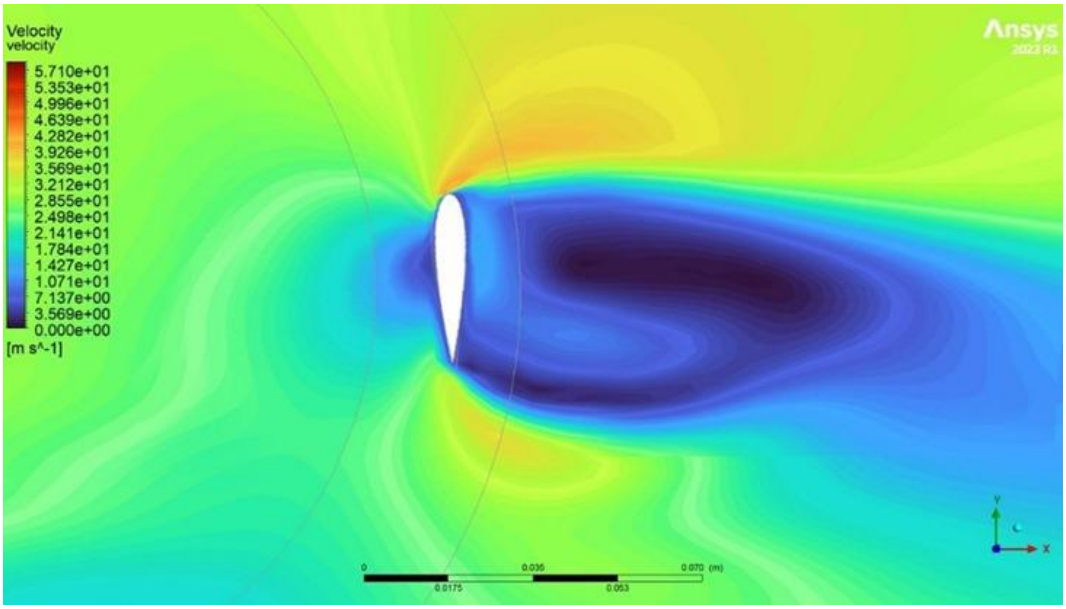

Figure 4.5: Air Flow Velocity Distributions at Air Velocity of 26 m/s, at θ=270°.

- **Streamlines colored by velocity magnitude for single blade**

The visualization of streamlines colored by velocity magnitude provides valuable insights into the flow characteristics of a Darrieus vertical axis wind turbine (VAWT) at various blade positions. Firstly, examining the streamlines for the blade positioned at 0° offers a depiction of

the flow pattern near the leading edge of the blade. This visualization enables the analysis of velocity distribution and the identification of regions with varying velocities. Secondly, investigating the streamlines corresponding to the blade positioned at 90° provides a distinct perspective, revealing the flow behavior around the trailing edge of the blade. This view facilitates the understanding of airflow separation, reattachment, and the formation of vortices. Additionally, a close-up view of the streamlines for the second blade at 90° allows for a detailed examination of the flow structure in close proximity to the blade surface, providing insights into boundary layer behavior and potential flow interactions. Lastly, exploring the streamlines for the blade positioned at 180° illustrates the flow dynamics on the opposite side of the rotor, showcasing differences in velocity magnitude and direction compared to other blade positions. As illustrated in Figure 4.6, 4.7, 4.8 and 4.9.

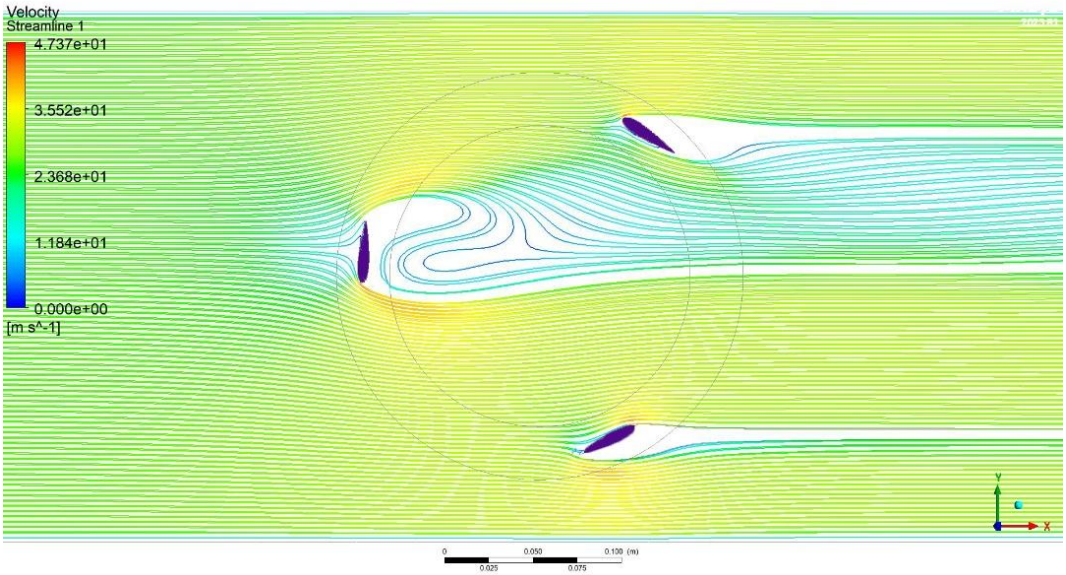

Figure 4.6: Streamlines Colored by Velocity Magnitude For Single Blade, at 9θ = 0°

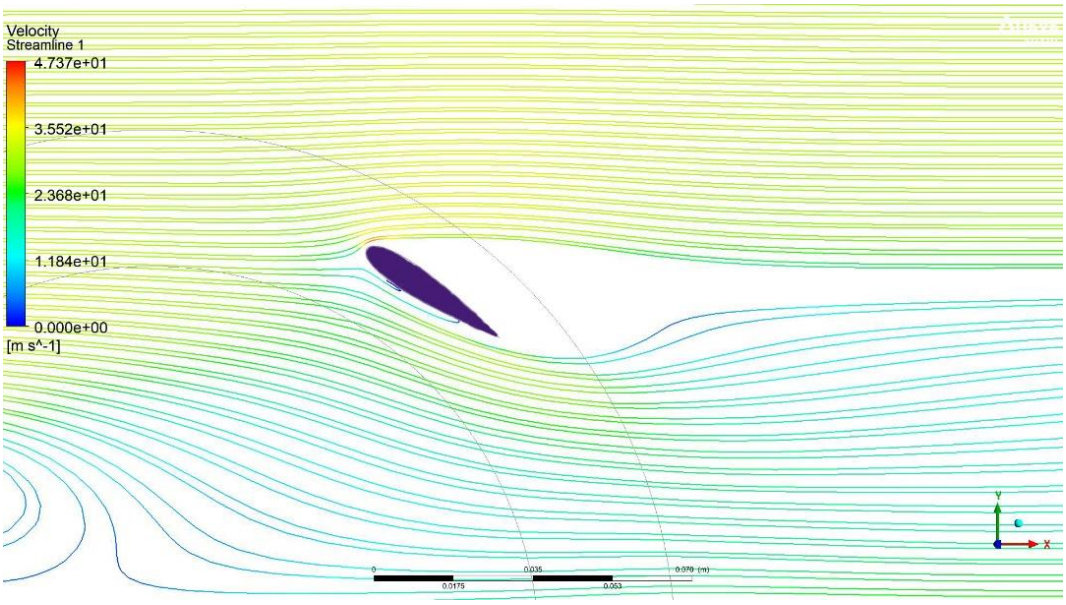

Figure 4.7: Streamlines Colored by Velocity Magnitude For Single Blade, at Same Position as illustrated in Figure 4.6 ,with close view at specific blade

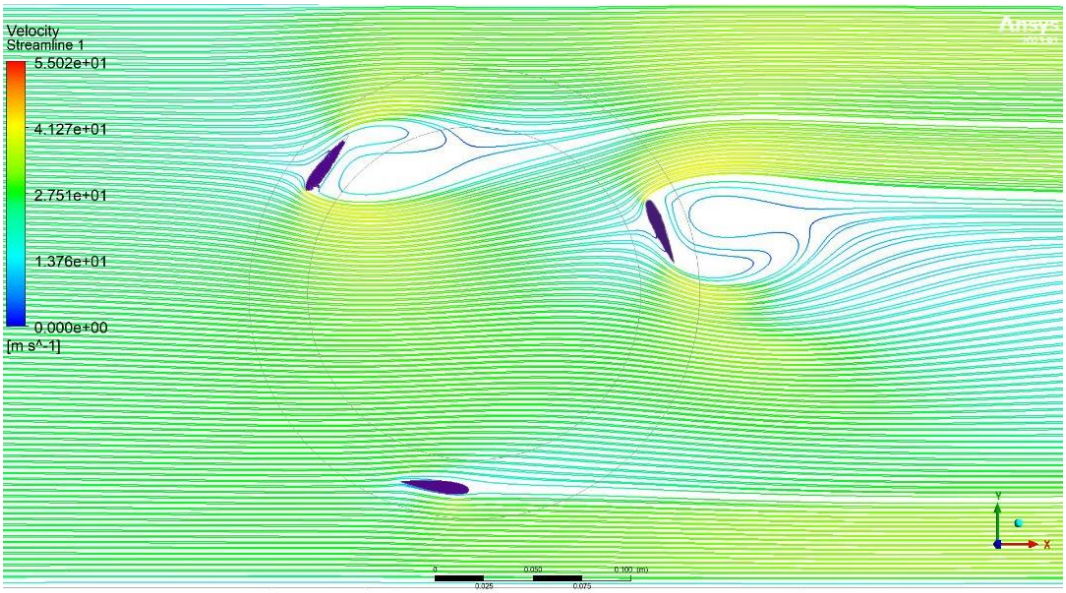

Figure 4.8: Streamlines Colored by Velocity Magnitude For Single Blade, at 18θ = 0°

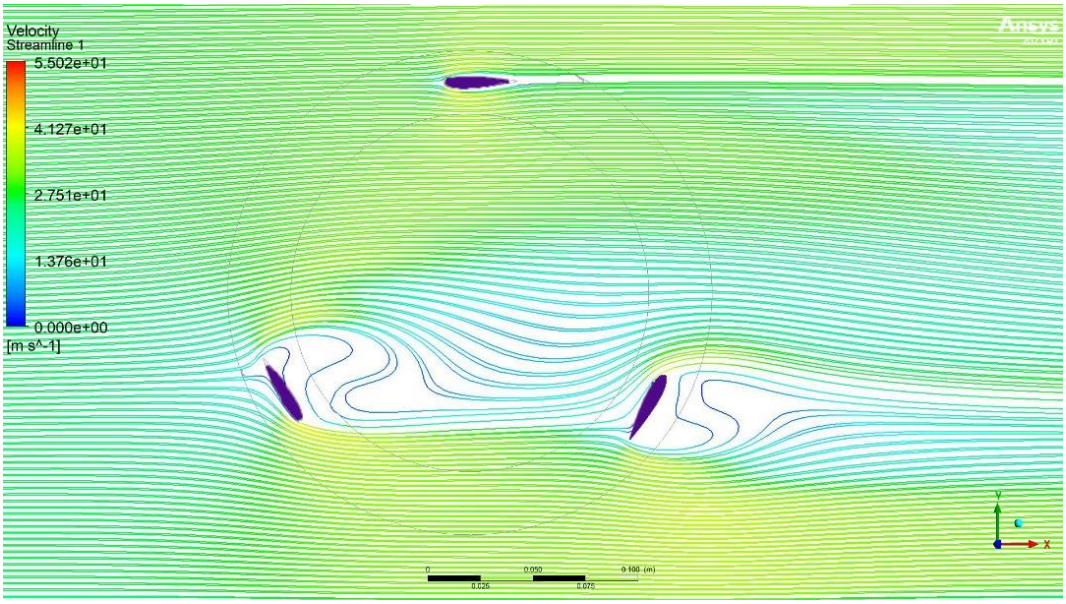

Figure 4.9: Streamlines Colored by Velocity Magnitude For Single Blade, at θ = 0°

4.1.1.3. Validation of numerical and experimental results for single blade

To assess the accuracy and reliability of the numerical simulations, a validation process was conducted by comparing the numerical results with the corresponding experimental data for the single blade configuration. The blade distance from the rotor was kept at 10 cm for both the numerical simulations and the experiments.

The power coefficient values obtained from the numerical simulations were compared with the experimental results, and the percentage error was calculated. The validation analysis revealed that the error range between the numerical and experimental results was approximately less than 20 % Error, which is considered reasonable for such complex aerodynamic simulations. Moreover, the trend observed in the power coefficient values from the numerical simulations was found to be compatible with the experimental results. validation between the numerical and experimental results shown in Figure 4.10.

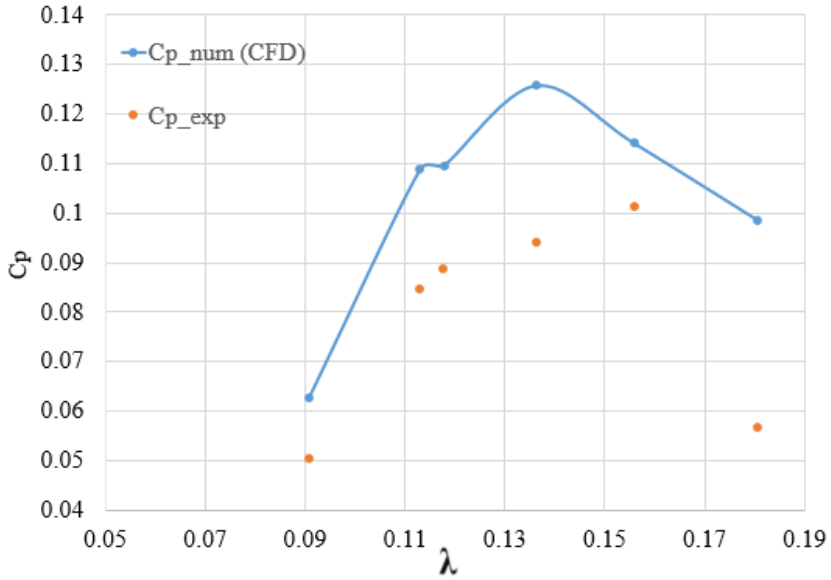

Figure 4.10: Validation Between the Numerical and Experimental Results.

The power coefficient values obtained from the numerical simulations range from 0.062547185 to 0.125840227. These results provide insights into the performance of the single blade configuration at different operating conditions.

The experimental results for the single blade configuration show power coefficient values ranging from 0.050447779 to 0.101276102. These results provide empirical data on the performance of the single blade design under different operating conditions.

This validation between the numerical and experimental results as illustrated in Figure 4.10 provides confidence in the accuracy of the numerical model in capturing the key aerodynamic characteristics of the single blade Darrieus wind turbine. The small percentage error and the good agreement in the overall trend of the power coefficient values demonstrate that the numerical simulations can effectively predict the performance of the single blade configuration.

4.1.2 Double Darrieus

This section is dedicated to the comprehensive analysis and discussion of the Double blade vertical axis wind turbines configuration.

4.1.2.1 Experimental results

Throughout this study, results were performed with different velocity for the double blade Darrieus wind turbine, the power coefficient values were evaluated for various inlet blade distances from the rotor. The outlet blade remained at a distance of 10 cm from the rotor. The

power coefficient values for different inlet blade distances (L) are presented in Figure 4.11, Figure 4.12, Figure 4.13, Figure 4.14 Figure 4.15 and Figure 4.16.

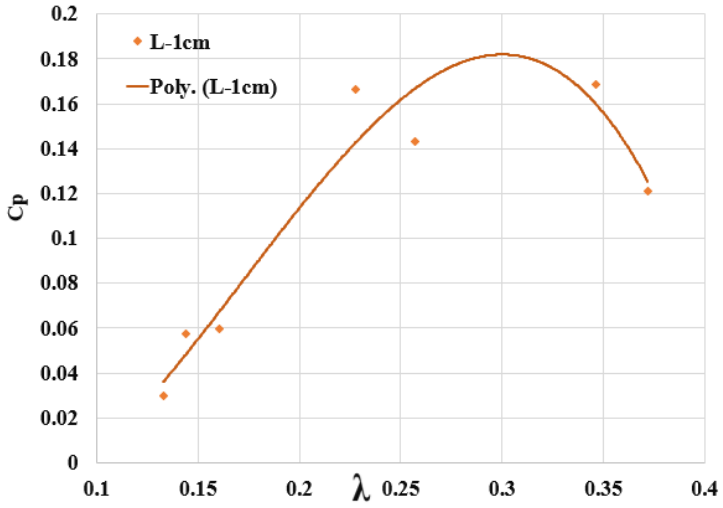

Figure 4.11: Power Coefficient Values For L=1 cm, L is Distances From Rotor To Inlet Blade.

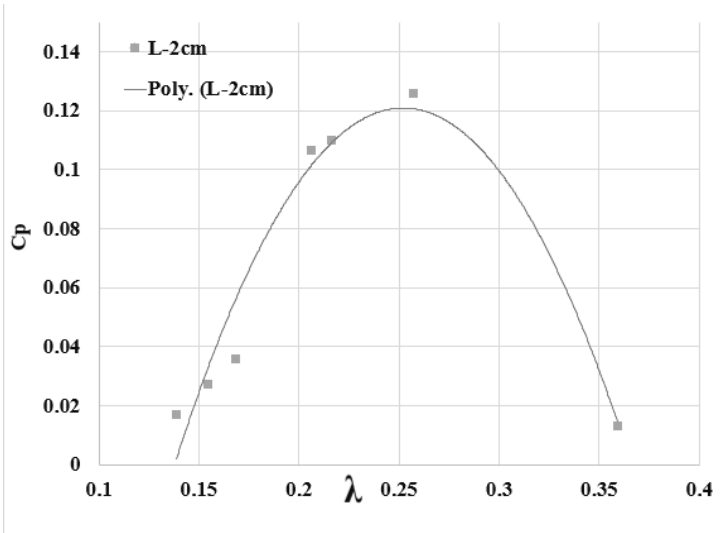

Figure 4.12: Power Coefficient Values For L=2 cm, L is Distances From Rotor To Inlet Blade.

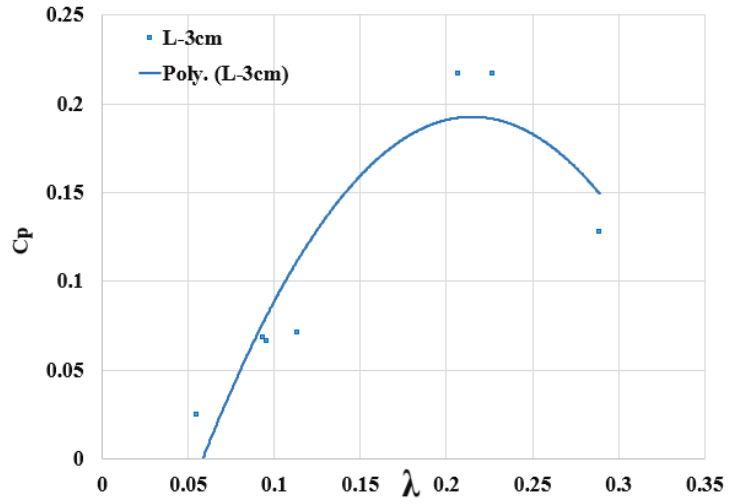

Figure 4.13: Power Coefficient Values For L=3 cm, L is Distances From Rotor To Inlet Blade.

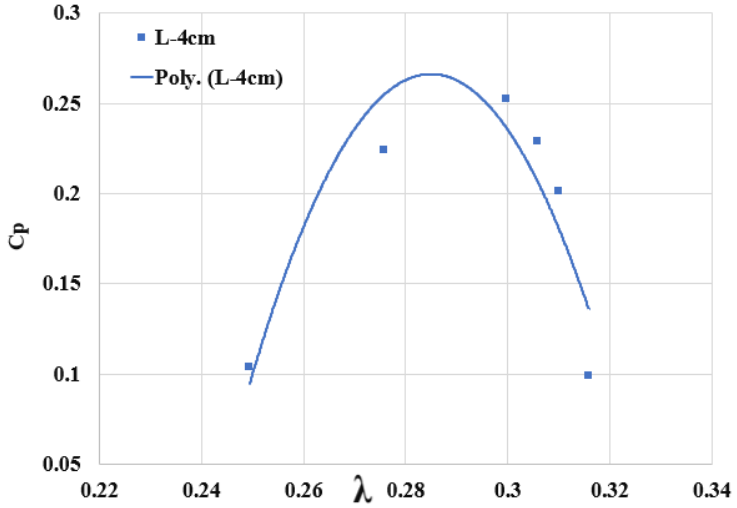

Figure 4.14: Power Coefficient Values For L=4 cm, L is Distances From Rotor To Inlet Blade.

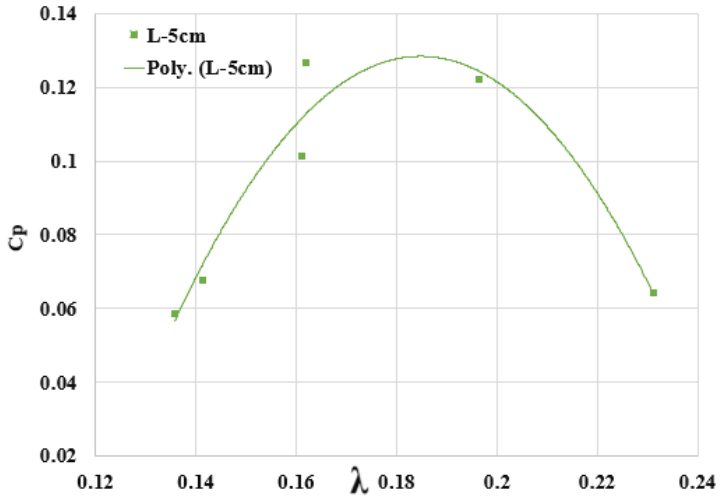

Figure 4.15: Power Coefficient Values For L=5 cm, L Distances From Rotor To Inlet Blade.

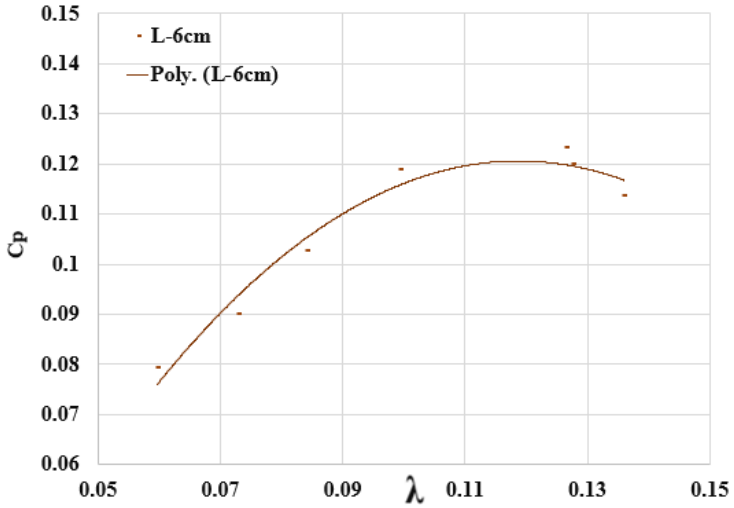

Figure 4.16: Power Coefficient Values For L=6 cm, L is Distances From Rotor To Inlet Blade.

The experimental results for double blade configuration provide insights into the effect of varying the inlet blade distance on the power coefficient. The power coefficient values vary for each inlet blade distance, ranging from 0.016711708 to 0.252215436. results showed that the most efficient position coincided with 40% of the length at 4 cm from rotor.

4.1.2.2 Numerical results

this section presents the numerical results obtained from the simulations of the double blade configuration of the Darrieus wind rotor. The simulations aimed to investigate the aerodynamic behavior and flow characteristics of this specific configuration. The results are analyzed and discussed in detail, providing insights into the performance of the double blade setup.

4.1.2.2 Air flow velocity distributions:

Contour plots of air flow velocity distributions were generated to visualize the variations in air velocities around the double blade configuration. Numerical results are obtained from the simulations of the double blade configuration of the Darrieus wind rotor. Contour depict air flow velocities around the double-blade setup at 26 m/s, aligning blades with wind flow (θ = 0°) results in even velocity distribution, ensuring effective wind energy use. Conversely, perpendicular blades (θ = 90°) lead to flow separation, wake effects, and decreased energy utilization. Notably, θ = 180° presents efficient configuration, while θ = 270° minimally affects power generation despite flow separation. Numerical results obtained from the simulations of the double blade shown in Figure 4.17, 4.18, 4.19 and 4.20.

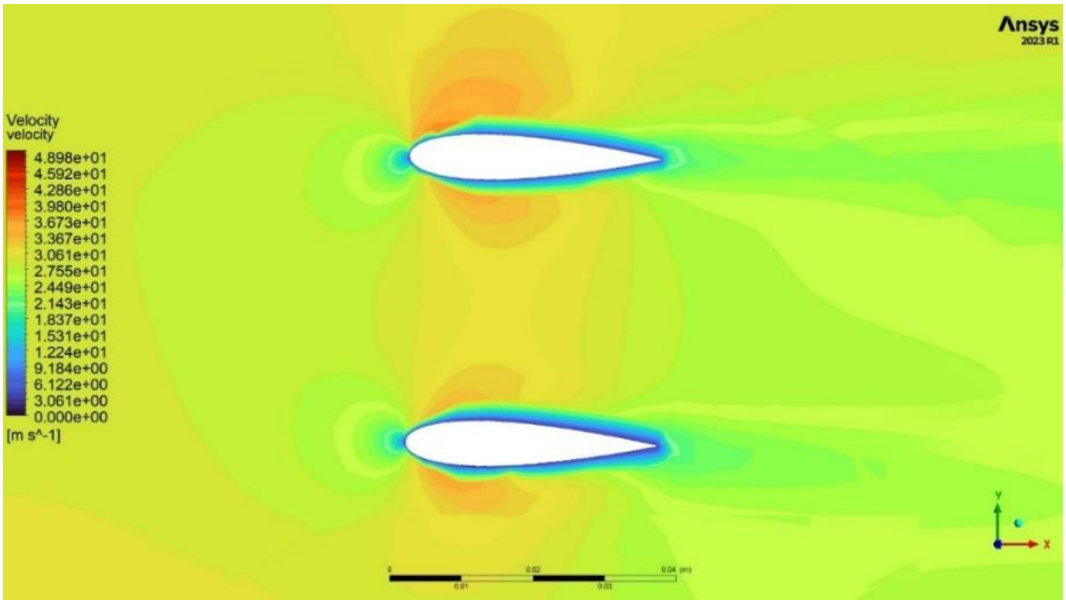

Figure 4.17: Air Flow Velocity Distributions at An Air Velocity Of 26 m/s, at θ = 0°

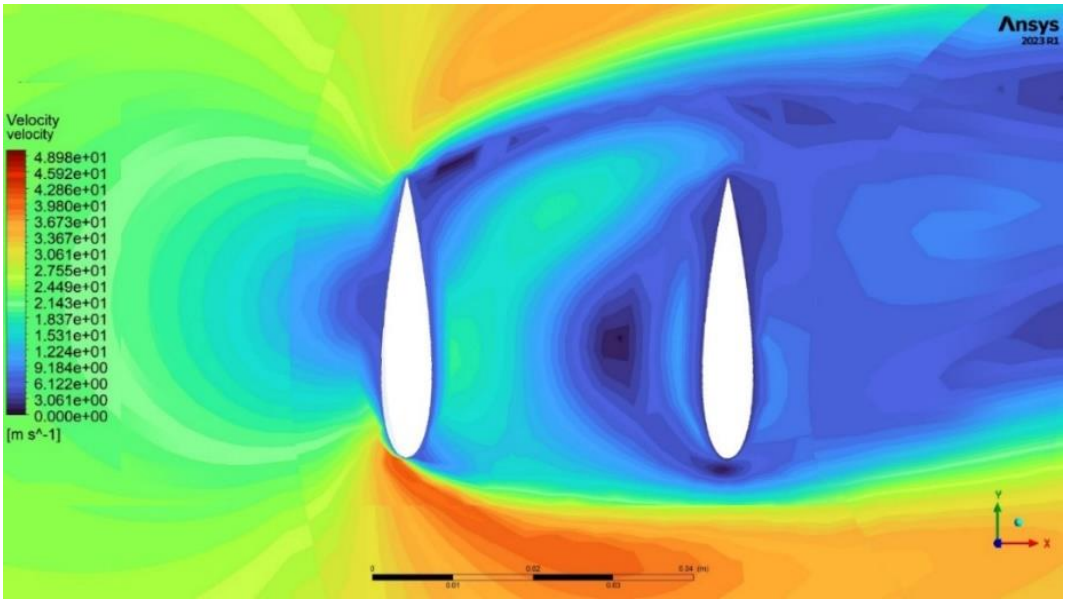

Figure 4.18: Air Flow Velocity Distributions at An Air Velocity Of 26 m/s, at θ =9 0°

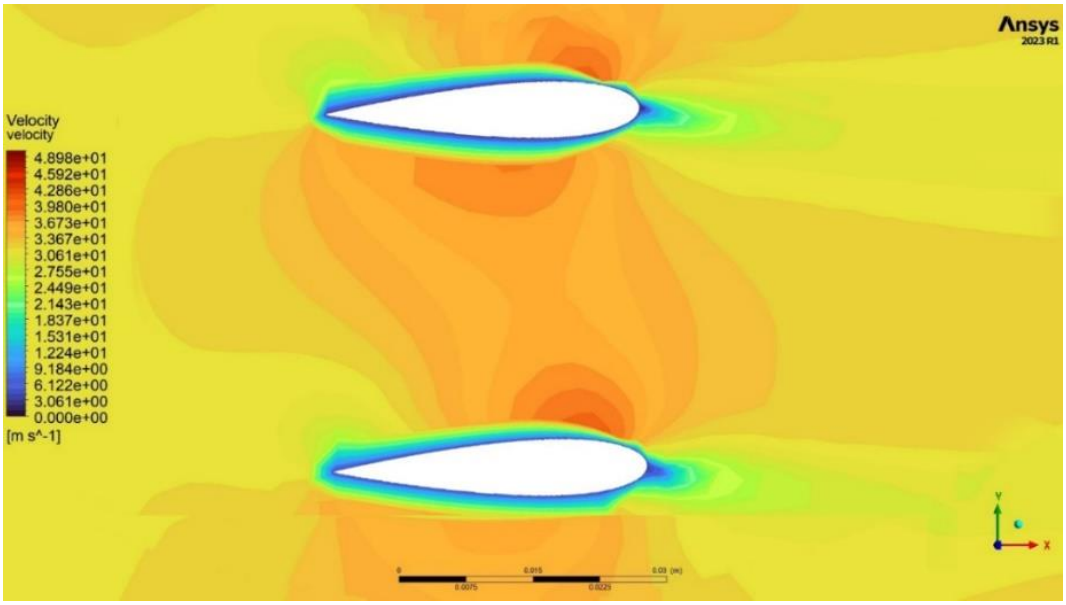

Figure 4.19: Air Flow Velocity Distributions at An Air Velocity Of 26 m/s, at θ =180°

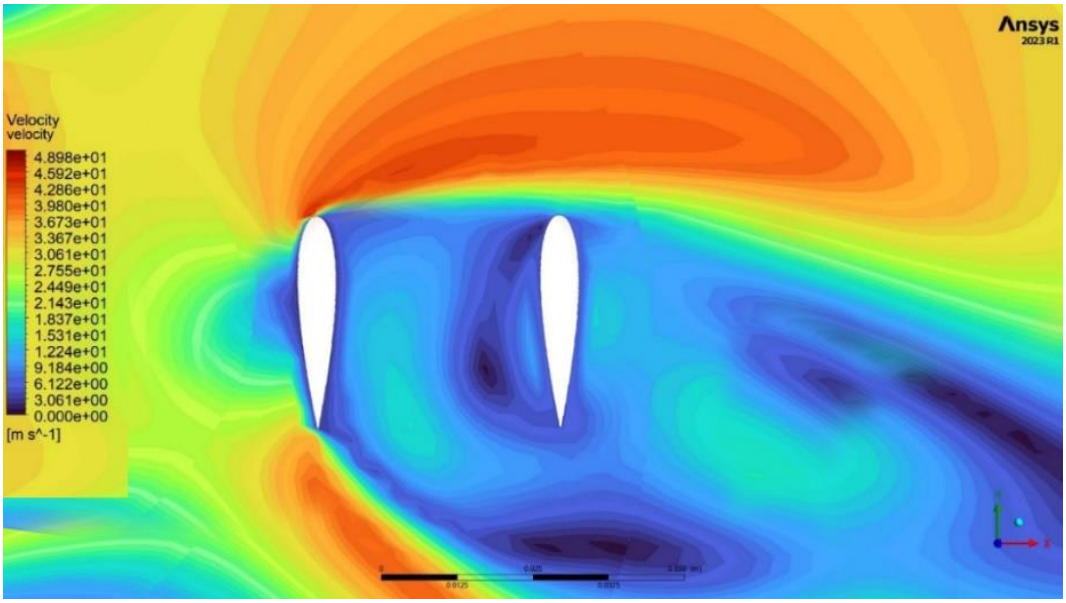

Figure 4.20: Air Flow Velocity Distributions at An Air Velocity Of 26 m/s, at θ=270°

4.1.2.3 Streamlines colored by velocity magnitude for double blade

The visualization of streamlines colored by velocity magnitude as illustrated in Figure 4.21, Figure 4.22, Figure 4.23 and Figure 4.24, provides valuable insights into the flow characteristics of a double-blade Darrieus vertical axis wind turbine (VAWT) at various blade positions. Examining the streamlines for the blade positioned at 0° offers a depiction of the flow pattern near the leading edge of the blade, allowing for the observation of velocity distribution and potential flow separation regions. The streamlines corresponding to the blade positioned at 90° provide a distinct perspective, revealing the flow behavior around the trailing edge of the blade and facilitating the understanding of airflow separation and vortices formation. Exploring the streamlines for the blade positioned at 180° showcases the flow dynamics on the opposite side of the rotor, highlighting differences in velocity magnitude and direction compared to other blade positions. Lastly, investigating the streamlines for the blade positioned close to 270° allows for a detailed examination of the flow structure near the trailing edge of the second blade, providing insights into boundary layer behavior and potential flow interactions in this region of the VAWT. Streamlines for double blade shown in Figure 4.22, Figure 4 .23, Figure 4 .24 and Figure 4 .25.

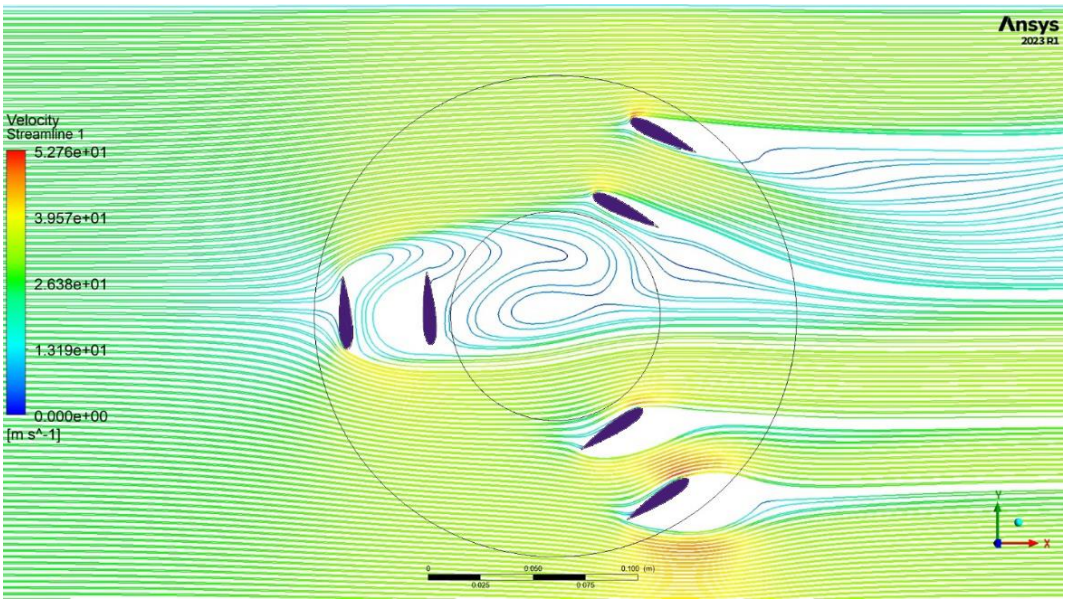

Figure 4.21: Streamlines Colored by Velocity Magnitude For Double Blade, at θ =90°.

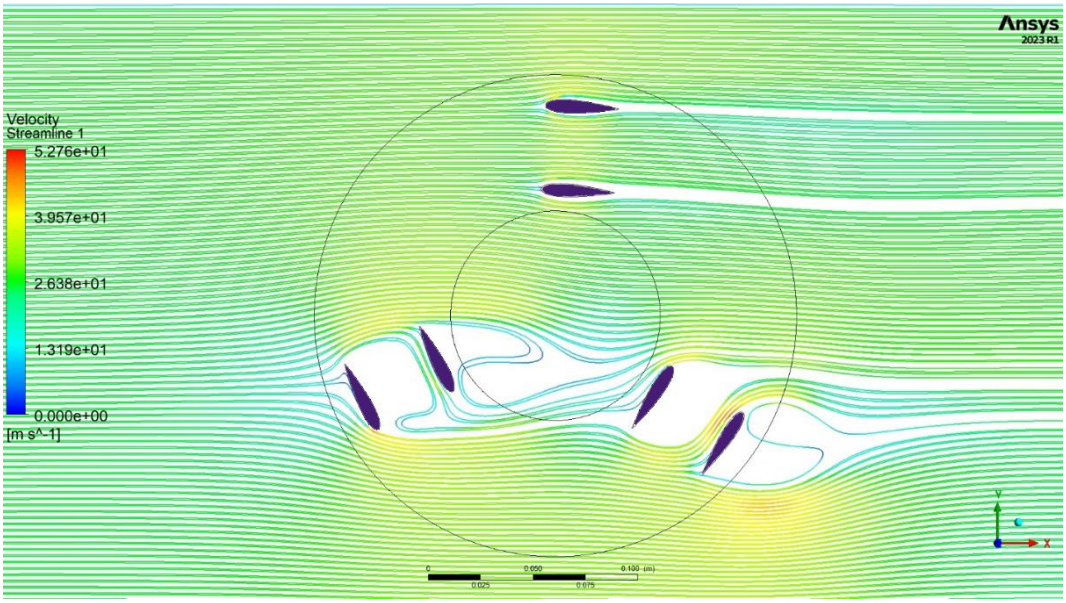

Figure 4.22: Streamlines Colored by Velocity Magnitude For Double Blade, at θ = 0°

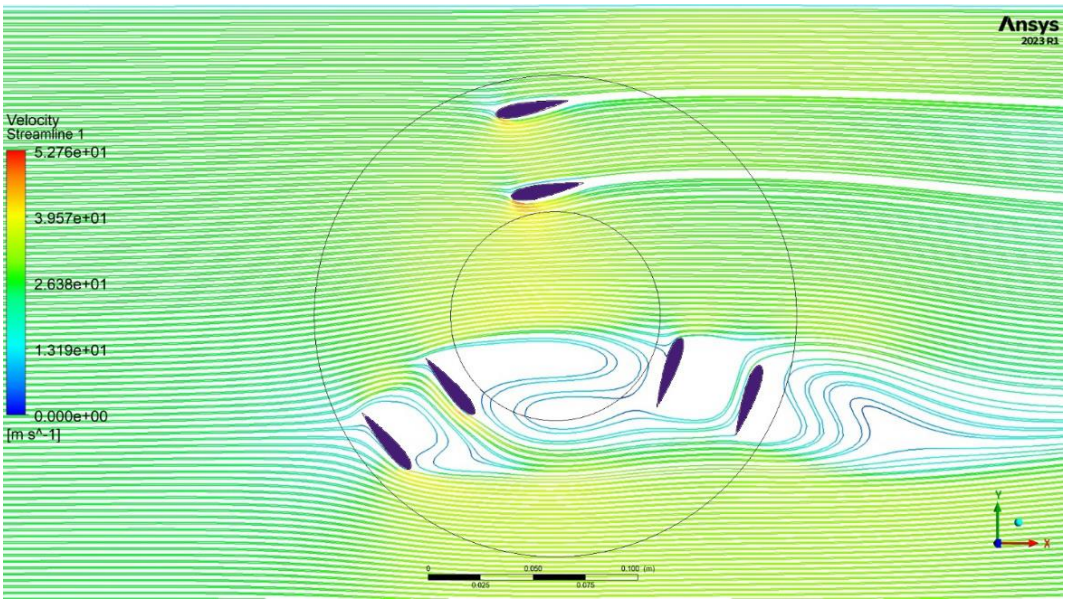

Figure 4.23: Streamlines Colored by Velocity Magnitude For Double Blade, at θ=245°

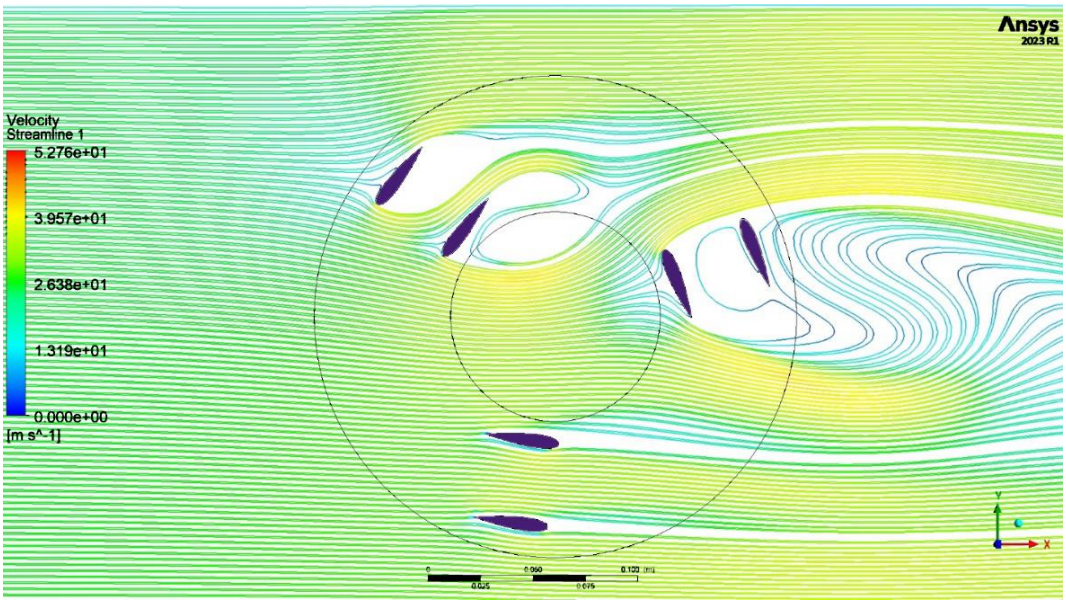

Figure 4.24: Streamlines Colored by Velocity Magnitude For Double Blade, at θ = 180°.

4.2 Discussion

This section presents the analysis of the Power Coefficient for Double-Bladed Darrieus Turbine, including an investigation of the optimal position for maximizing the power coefficient. Furthermore, a comparative analysis between the numerical results of Double-Bladed and Single-Bladed Darrieus Turbines is conducted to assess their respective performance. Additionally, the relationship between the Tip Speed Ratio of the Darrieus Wind Turbine and its solidity is analyzed. Lastly, the application of the similarity equation is explored, aiming to establish a correlation between the velocities measured in wind tunnels and the velocities encountered by wind turbines in real-world operating conditions.

4.2.1 A Comparison between Double and Single Blade Darrieus wind turbine

After simulating the single blade Darrieus wind turbine and the double blade Darrieus wind turbine using ANSYS software, a comprehensive comparison between the two cases was conducted. The objective of this comparison was to assess the performance improvement achieved by the double blade configuration and to validate the numerical results against the experimental data. By analyzing and comparing the aerodynamic characteristics, power coefficients, and flow patterns obtained from both simulations, valuable insights were gained regarding the effectiveness of the double blade design. As mentioned in section 4.1.1.2 Numerical Results for single blade 4.2.2 Numerical results for double blade and Figure 4.16 where the blade at 5 cm from the rotor and at a speed of 26 m/s. the result for single blade power coefficient (Cp) is 0.108, and the results for Double blade power coefficient (Cp) is 0.117, this indicate Improvement of 6.7% between single blade and double blade numerical cases.

4.2.2 Power Coefficient Analysis for Double-Blade Darrieus Turbine

The power coefficient analysis for the double-blade Darrieus turbine showed in section Experimental results Figure 4.14 and Figure 4.15 revealed the influence of blade positioning on the turbine's performance. The power coefficient values varied with the distance of the inlet blades from the rotor, indicating the importance of blade placement for maximizing power extraction. The results showed that the power coefficient generally increased as the inlet blade distance decreased especially from 30% to 40% distance from the rotor.

CHAPTER FIVE

CONCLUSION AND FUTURE WORKS

5.1 Conclusion

This study has explored the potential of wind energy as a clean and renewable source of power, highlighting its importance in addressing environmental concerns on fossil fuels. The experimental and numerical study conducted on the double-blade Darrieus wind turbine has provided valuable insights into its performance and flow characteristics.

- The analysis of power coefficient and tip speed ratio has shed light on the influence of blade positioning and design parameters on turbine performance, results showed that the most efficient position coincided with 40% and 30% of the length.

- The comparison between single blade and double blade numerical cases Results showed an Improvement of 6.70% in Power coefficient for Double Blade.

The insights gained from the experimental and numerical study can be utilized to optimize the design, operation, and integration of double-blade Darrieus turbines for enhanced wind energy utilization.

In conclusion, this thesis has provided insights into wind energy potential, the performance of double-blade Darrieus turbines, and the comparison between numerical and experimental results.

5.2 Future Works

Building upon the findings of this thesis, several avenues for future research and development in the field of wind energy can be explored:

- Experimental: Continued experimental validation of the Double Darrieus Blade, but this time with an offset configuration instead of a Parallel configuration.

- Numerical Modeling: Continued Numerical simulation but this time with an offset configuration instead of a Parallel configuration.

- Continued the study with changes in solidity and blade shape.

REFERENCES

1. Manwell, J.F., McGowan, J.G., Rogers, A.L. Wind Energy Explained: Theory, Design and Application. Hoboken, NJ: John Wiley & Sons. (2010).
2. David A. WIND TURBINE TECHNOLOGY Fundamental Concepts oF Wind turbine engineering (2nd ed.).2009.
3. Bošnjaković, M., Katini´c, M., Santa,R., Mari´c, D., " Wind Turbine Technology Trends", Applied Sciences., 12(17):8653, 2022
4. Li, Y., Straight-bladed vertical axis wind turbines: history, performance, and applications. 2019.
5. Kumar, P.M, Sivalingam, K., Narasimalu, S., Lim,T., Ramakrishna, S., Wei.H., " A review on the evolution of darrieus vertical axis wind turbine: Small wind turbines" . Journal of Power and Energy Engineering. 7(4): p. 27-44. 2019
6. Ghasemian, M. , Ashrafi, Z. N. , Sedaghat, A., "A review on computational fluid dynamic simulation techniques for Darrieus vertical axis wind turbines", Energy Conversion and Management, 149: p. 87-100. 2017
7. Islam, M., David S.-K. Ting, Fartaj, A., "Aerodynamic models for Darrieus-type straight-bladed vertical axis wind turbines". Renewable and Sustainable Energy Reviews, , 12(4): p. 1087-1109 . 2008
8. Bangga, G., Dessoky,A.,Wu, Z., Rogowski, K., and Hansen, M., " Accuracy and consistency of CFD and engineering models for simulating vertical axis wind turbine loads" . , Energy , 206: p. 118087. 2020.
9. Beri, H., Yao, Y., "Double multiple streamtube model and numerical analysis of vertical axis wind turbine" Energy and Power Engineering, 3,p. 262-270 , 2011 .
10. Brusca, S., Lanzafame, R., Messina, M., "Design of a vertical-axis wind turbine: how the aspect ratio affects the turbine's performance" . 5(4): p. 333-340. 2014.
11. Jekabsons, N., Upnere, S., Kleperis, J., "numerical and experimental investigation of h-darrieus vertical axis wind turbine", engineering for rural development, jelgava, 25.-27.05.2016
12. Bianchini , A., Balduzzi,F., Bachant,P., Ferrara, G., Ferrari,L., "Effectiveness of two-dimensional CFD simulations for Darrieus VAWTs: a combined numerical and experimental assessment" . Energy Conversion and Managemen, 136: p. 318-328. 2017.

13. Cai,X., Zhang,Y. , Ding, W. , and Bian, S., “The aerodynamic performance of H-type darrieus VAWT rotor with and without winglets: CFD simulations.”, Energy Sources, Part A: Recovery, Utilization, and Environmental Effects, : p. 1-12 , 2019
14. singh Biswas,S., Biswas, A., “Investigation of self-starting and higH-Darrieus solidity on the performance of a three S1210 blade H-type Darrieus rotor” . Energy Conversion and Management 87 ,859-867, 2014
15. Soultanzadeh, B., Morad, A., “Numerical simulation and experimental study of blade pitch effect on Darrieus straight-bladed wind turbine with high solidity”. SN Applied Sciences, 3(4): p. 1-13. 2021.
16. Firdaus, R., KIWATA, T., KONO, T., NAGAO, K., “Numerical and experimental studies of a small vertical-axis wind turbine with variable-pitch straight blades”, Journal of Fluid Science and Technology, 10(1): p. JFST0001-JFST0001. 2015.
17. Gaikwad, S. , Patil, V. , Patil, A. , Kulkarni R.S. , “A Review on the Savonius VAWT”, International Research Journal of Engineering and Technology (IRJET)” (e-ISSN: 2395-0056 , 2017.
18. Kadam, A., Patil, S. , “A review study on Savonius wind rotors for accessing the power performance”., Second National Conference on Recent Developments in Mechanical Engineering M.E.Society's College of Engineering, Pune, India , 5: p. 18-24. 2013.
19. Roy, S. and Saha , U. K. , “Computational study to assess the influence of overlap ratio on static torque characteristics of a vertical axis wind turbine”, Procedia Engineering , 51: p. 694-702. 2013.
20. Ali, M., “ Experimental comparison study for Savonius wind turbine of two & three blades at low wind speed” , International Journal of Modern Engineering Research (IJMER), 3(5): p. 2978-2986. 2013.
21. Mahmoud, N.H., El-Haroun A.A., Wahba, E. ,Nasef, M.H., “ An experimental study on improvement of Savonius rotor performance”. , Alexandria Engineering Journal, 51(1): p. 19-25. 2012.
22. Sawla, A., Baredar, P., Manjhi, V. K., “ Computational Analysis of Vertical Axis Savonius Rotor”. (International Research Journal of Engineering and Technology (IRJET) e-ISSN: 2395 -0056 Volume: 03 Issue: 06 | June-2016 www.irjet.net p-ISSN: 2395-0072) 2016.
23. Widodo, W., Chin, A.C., SIHOMBING, H., YUHAZRI, M.Y., “Design and analysis of 5 kW Savonius rotor blade”., Global Engineers & Technologists Review, 2(8): p. 1-8. 2012.

24. Dobrev, I. , Massouh, F., “CFD and PIV investigation of unsteady flow through Savonius wind turbine”. , Energy Procedia , 6: p. 711-720. 2011.
25. Sharma, K.K., Gupta, R., Biswas, A., “Performance measurement of a two-stage two-bladed Savonius rotor”. , INTERNATIONAL JOURNAL of RENEWABLE ENERGY RESEARCH 4(1): p. 115-121. , 2014.
26. Maldonado, R. D., Huerta, E., Corona, J. E., Ceh, O., León-Castillo, A. I., Gómez-Acosta, M. P., Mendoza-Andrade, E., “Design, simulation and construction of a Savonius wind rotor for subsidized houses in Mexico”, Energy Procedia, 57: p. 691-697. 2014.
27. Irabu, K., Roy, J. N., “Characteristics of wind power on Savonius rotor using a guide-box tunnel.” , Experimental Thermal and Fluid Science 32(2): p. 580-586. , 2007.
28. Patel C.R., Patel V.K., Prabhu S.V., Eldho T.I., “Investigation of overlap ratio for Savonius type vertical axis hydro turbine”, International Journal of Soft Computing and Engineering (IJSCE) , 3(2): p. 379-383. 2013.
29. Wahyudi, B., Soeparman S., Wahyudi S., and Denny W. , “ A simulation study of Flow and Pressure distribution patterns in and around of Tandem Blade Rotor of Savonius (TBS) Hydrokinetic turbine model”, Journal of Clean Energy Technologies1(4): p. 286-291. , 2013.
30. Rainbird,J.M., Bianchini, A., Balduzzi, F., Peiró, J., Graham, J.M., Ferrara,G., Ferrari,L, “On the influence of virtual camber effect on airfoil polars for use in simulations of Darrieus wind turbines”. Energy Conversion and Management , 106: p. 373-384. 2015.
31. Chaitep ,S., Chaichana , T., Watanawanyoo, P., Hirahara, H., “Performance evaluation of curved blades vertical axis wind turbine”, European Journal of Scientific Research, 57(3): p. 435-446. 2011.
32. Matrawy K.K., Aly, A., A., Mahrous, A-F., “Performance evaluation of vertical axis wind turbine with a leading edge flap.”, International Journal of Control, Automation And Systems, 3(4) 2014.
33. Loya, A., Khan, M.Z., Bhutta, R.A., Saeed, M., “Dependency of torque on aerofoilcamber variation in vertical axis wind turbine”, World Journal of Mechanics , 6(11): p. 472-486. 2016.
34. Iham F. Zidane, Hesham M. Ali, Greg Swadener, Yehia A. Eldrainy, Ali I. Shehata, “Effect of upstream deflector utilization on H-Darrieus wind turbine performance: An

optimization study.” Alexandria Eng. J. (2022), Volume 63, 15 January 2023, Pages 175-189

35. Bashar, M.M., “Computational and Experimental Study on Vertical Axis Wind Turbine in Search for an Efficient Design.”, Electronic Theses and Dissertations , 1184, 2014.
36. Howell, R., Qin, N., Edwards, J., Durrani, N., “Wind tunnel and numerical study of a small vertical axis wind turbine”, Renewable Energy , 35(2): p. 412-422. 2010.
37. Rahman, M., Ahmed,M., Bashar,M., Mitra,A., Salyers,T., “Numerical and Experimental Investigations on Vertical Axis Wind Turbines of Different Models” . OALib Journal, 4(01): p. 1.2017.
38. Rahman,M., Salyers,T., El-Shahat,A., Ilie,M., Ahmed,M., Soloiu,V., “Numerical and Experimental Investigation of Aerodynamic Performance of Vertical-Axis Wind Turbine Models with Various Blade Designs” ., Journal of Power and Energy Engineering, 6(5): p. 26-63. 2018.
39. Alaimo , A., Esposito, A., Messineo, A., Orlando, C., Tumino, D., “3D CFD analysis of a vertical axis wind turbine.”, Energies , 8(4): p. 3013-3033. 2015.
40. Parker, C.M. Leftwich, M.C., “The effect of tip speed ratio on a vertical axis wind turbine at high Reynolds numbers”, Exp Fluids , 57(5): p. 1-11. (74) 2016.
41. Rezaeiha, A., Kalkman, I., Blocken, B., “CFD simulation of a vertical axis wind turbine operating at a moderate tip speed ratio: Guidelines for minimum domain size and azimuthal increment”, Renewable Energy , 107: p. 373-385. 2017.
42. Rezaeiha, A., Montazeri, H., Blocken, B., “Towards accurate CFD simulations of vertical axis wind turbines at different tip speed ratios and solidities: Guidelines for azimuthal increment, domain size and convergence”, Energy Conversion and Management , 156: p. 301-316. 2018.
43. Burlando, M., Ricci, A., Freda, A., Repetto, M.P., “Numerical and experimental methods to investigate the behaviour of vertical-axis wind turbines with stators”, Journal of Wind Engineering.year
44. Smily, J., Radi, B., “Probabilistic Study of S809 Airfoil for Wind Turbine Blade”., Advances in Theoretical and Applied Mechanics, 13(1): p. 1-9. 2021.
45. Hansen, J.T., Mahak, M., and Tzanakis, I., “Numerical modelling and optimization of vertical axis wind turbine pairs: A scale up approach.”, Renewable Energy, 171: p. 1371-1381. 2021.

46. Altmimi, A., Alaskari, M. , Abdullah, O. I. , Alhamadani, A., Sherza, J. , “Design and Optimization of Vertical Axis Wind Turbines Using QBlade”, Applied System Innovation , 4(4): p. 74. 2021.
47. Unsakul, S., Sranpat, C., Chaisiriroj, P., Leephakpreeda, T., “CFD-based performance analysis and experimental investigation of design factors of vertical axis wind turbines under low wind speed conditions in Thailand”, Journal of Flow Control, Measurement & Visualization, 5(04): p. 86-98.2017.
48. Rossetti, A., Pavesi, G., “Comparison of different numerical approaches to the study of the H-Darrieus turbines start-up.”, Renewable Energy, 50: p. 7-19. 2013.
49. Asr, M.T., Nezhad, E.Z., Mustapha, F. , Wiriadidjaja, S., “Study on start-up characteristics of H-Darrieus vertical axis wind turbines comprising NACA 4-digit series blade airfoils”., Energy, 112: p. 528-537. 2016.
50. Celik, Y. , Maa, L., Inghama, D., Pourkashanian, M., “Aerodynamic investigation of the start-up process of H-type vertical axis wind turbines using CFD”, Journal of Wind Engineering and Industrial Aerodynamics, 204: p. 104252. 2020.
51. Untaroiu, A., et al., Investigation of self-starting capability of vertical axis wind turbines using a computational fluid dynamics approach. 133(4). 2011.
52. Zhu, J., Huang, H., Shen, H., “Self-starting aerodynamics analysis of vertical axis wind turbine”, Advances in Mechanical Engineering , 7(12) 1-12 : p. 1687814015620968. 2015.
53. Worasinchai, S., Ingram, G., Dominy, R., “Effects of wind turbine starting capability on energy yield”, Journal of Engineering for Gas Turbines and Power, 134(4). 2012.
54. Zhu, J.-y., Jiang L., Zhao, H., “Effect of wind fluctuating on self-starting aerodynamics characteristics of VAWT”, J. Cent. South Univ , 23(8): p. 2075-2082. 2016.
55. Worasinchai, S., “Small wind turbine starting behavior”., paper , Durham University, 2012.
56. Bhuyan, S., Biswas, A., “ Investigations on self-starting and performance characteristics of simple H and hybrid H-Savonius vertical axis wind rotors”, Energy Conversion and Management , 87: p. 859-867. 2014.
57. Hosseini, A., Goudarzi, N., “Design and CFD study of a hybrid vertical-axis wind turbine by employing a combined Bach-type and H-Darrieus rotor systems”, Energy Conversion and Management , 189: p. 49-59, 2019.
58. El-Nenaey,K., et al., Performance Evaluation of Hybrid Vertical Axis Wind Turbine.

59. Hammond, O., Hunt, S., Machlin, E., “Design of an alternative hybrid vertical axis wind turbine” , paper, 2014
60. Mohammed, G., Ibrahim, A., Kangiwa, U. M., Wisdom, J. B., “Design and Testing of Building Integrated Hybrid Vertical Axis Wind Turbine”, Journal of Electrical and Electronic Engineering, 9(3): p. 69-77. 2021.
61. Pallotta, A., Pietrogiacomi, D. , Romano, G.P., “ HYBRI–A combined Savonius-Darrieus wind turbine: Performances and flow fields”, Energy ,191: p. 116433. ,2019, 2020.
62. Alam, M.J., Iqbal, M.T., “Design and development of hybrid vertical axis turbine. in 2009 Canadian conference on electrical and computer engineering.” IEEE. 2009.
63. Ahmad, M., Shahzad, A., Akram , F., Ahmad , F., Shah, S. I. A, “Design optimization of Double-Darrieus hybrid vertical axis wind turbine”, Ocean Engineering , 254: p. 111171, 2022.
64. Kumar,P. M. , Ajit, K. , Surya, M. , Srikanth, N., Lim, T. , “On the self starting of darrieus turbine: An experimental investigation with secondary rotor”. in 2017 Asian Conference on Energy, Power and Transportation Electrification (ACEPT). IEEE, 2017.
65. Dabiri, J. O. Potential order-of-magnitude enhancement of wind farm power density via counter-rotating vertical-axis wind turbine arrays. Journal of Renewable and Sustainable Energy, 3(4), 043104. 2011
66. E. Saber a, R. Afify a, H. Elgamal b., “Performance of SB-VAWT using a modified double multiple streamtube model.” Alexandria Eng. J. (2018)
67. Lanzafame, R., Mauro,S., Messina,M., Brusca,S., “Development and Validation of CFD 2D Models for the Simulation of Micro H-Darrieus Turbines Subjected to High Boundary Layer Instabilities” ,Energies, 13, 5564, 2020.

APPENDIX

APPENDIX A: Arduino Code

Code for Arduino for load cell and speed sensor

```
//Load Cell 20k
#include "HX711.h"
#define calibration_factor 109.75 //108 //106.5
#define DOUT  7
#define CLK  6
HX711 scale;//(DOUT, CLK);
const int NumOfReading=100;
float loadArray[NumOfReading], LoadAVG=0.0, LoadSum=0.0;
//Encoder float p=0.0,TOV=0.0,Sum_RPM=0.0; const byte interruptPin = 2; void setup() {
  //Load Cell 20k
  Serial.begin(9600); scale.begin(DOUT, CLK);
  Serial.println("HX711 scale"); scale.set_scale(calibration_factor);
//This value is obtained by using the SparkFun_HX711_Calibration sketch  scale.tare();
//Assuming there is no weight on the scale at start up, reset the scale to 0
  Serial.println("Readings:"); for(int i=0;i<NumOfReading;i++)loadArray[i]=0.0;
  // Encoder sei(); Setup_Timer1();
  pinMode(2, INPUT);  digitalWrite(2, HIGH);       // turn on pullup resistors
  Serial.println("wellcome");  pinMode(interruptPin, INPUT_PULLUP);
  attachInterrupt(digitalPinToInterrupt(interruptPin), Encoder, RISING);
void loop() for(int i=NumOfReading-1; i>0; i--)loadArray[i]=loadArray[i-1];
    loadArray[0]=scale.get_units();  LoadSum=0.0;
```

```
   for(int i=0;i<NumOfReading;i++) LoadSum+=loadArray[i];
   LoadAVG=LoadSum/NumOfReading;
 //Encoder  if(TOV>=20){ Serial.print("R:");
 Serial.print(Sum_RPM*0.5);//////////////AVG_RPM*0.3*20 where 0.3 --> 200ms to 1min and
1rev =600pluse Serial.print("F:");
 Serial.println(LoadAVG);// Load Cell TOV=0    p=0;  Sum_RPM=0;


void Setup_Timer1(){
  // Timer/Counter 1 initialization
  // Clock source: System Clock
  // Clock value: 2000.000 kHz
  // Mode: Normal top=0xFFFF
  // OC1A output: Disconnected
  // OC1B output: Disconnected
  // OC1C output: Disconnected
  // Noise Canceler: Off
  // Input Capture on Falling Edge
  // Timer Period: 10 ms
  // Timer1 Overflow Interrupt: On
  // Input Capture Interrupt: Off
  // Compare A Match Interrupt: Off
  // Compare B Match Interrupt: Off
  // Compare C Match Interrupt: Off
  TCCR1A=0x00;
```

```
  TCCR1B=(0<<ICNC1) | (0<<ICES1) | (0<<WGM13) | (0<<WGM12) | (0<<CS12) | (1<<CS11) | (0<<CS10);

  TCNT1H=0xB1;

  TCNT1L=0xE0;

  ICR1H=0x00;

  ICR1L=0x00;

  OCR1AH=0x00;

  OCR1AL=0x00;

  OCR1BH=0x00;

  OCR1BL=0x00;

//  OCR1CH=0x00;

//  OCR1CL=0x00;

  // Timer/Counter 1 Interrupt(s) initialization

  TIMSK1=  (0<<ICIE1) | (0<<OCIE1B) | (0<<OCIE1A) | (1<<TOIE1);  //(0<<ICIE1) | (0<<OCIE1C) | (0<<OCIE1B) | (0<<OCIE1A) | (1<<TOIE1);

//Timer 1 Interrupt Code ISR(TIMER1_OVF_vect){

  // Reinitialize Timer1 value  TCNT1H=0xB1E0 >> 8;  TCNT1L=0xB1E0 & 0xff;

  // Place your code here  TOV++; Sum_RPM+=p   p=0; } void Encoder() {
```

APPENDIX B: Load Cell Calibration Curve

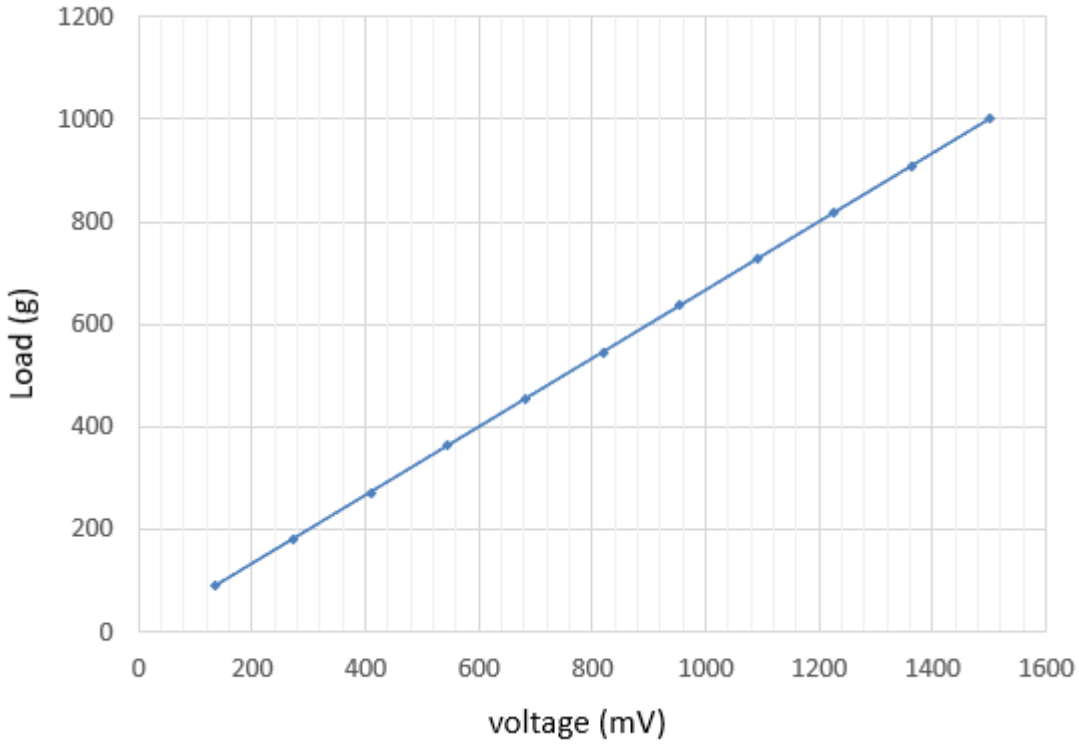

Figure: Load Cell Calibration Curve

ملخص الرسالة

يقدم هذا البحث تحقيقًا شاملاً في الأداء والخصائص الديناميكية الهوائية لتوربينات الهواء من نوع داريوس بمجموعتين من الريش كلاهما من نوع **NACA 0018** . تستخدم الدراسة نهجاً مزدوجا، يجمع بين تجربة نفق الرياح والمحاكاة العددية التي يسهلها برنامج الانسيس، لفحص سلوك التوربينات في ظل ظروف الرياح المختلفة. تشمل القياسات التجريبية عزم الدوران وإنتاج الطاقة، في حين أن عمليات محاكاة ديناميكيات الموائع الحسابية توفر أنماط التدفق وتوزيع الضغط.

تظهر النتائج بشكل واضح وجود توافق وثيق بين نتائج التجريبية والعددية، مما يؤكد دقة النموذج الحسابي. بالإضافة إلى ذلك، يؤكد التحليل على التأثير العميق لسرعة الرياح على أداء التوربينة مما يسلط الضوء على السمات الديناميكية الهوائية المفيدة للريشة **NACA 0018** .

تقدم هذه النتائج مساهمات جوهرية في مجال تحسين أداء توربينات الرياح وتقدم رؤى قيمة لها آثار على الأبحاث القادمة في مجال الطاقة المتجددة. علاوة على ذلك، يحدد هذا البحث التكوين الأمثل في المنهج التجريبي لتوربينات الرياح ذات المحور الرأسي داريوس ذات الريشة المزدوجة. أظهرت النتائج أن الموقع الأكثر كفاءة يقع على مسافة 4 سم و 3 سم من الدوار، وهو ما يعادل 40٪ إلى 30٪ من حيث نسبة المسافة. ومن الجدير بالذكر أنه لوحظ تحسن بنسبة 6.7% عند مقارنة النتائج الرقمية للريشة المفردة والريشة المزدوجة.

إقرار لجنة التحكيم والمناقشة

إسم الدارس

تم مناقشة هذه الرسالة وإجازتها بتاريخ: / /

أعضـاء اللجنـة

الأساتذة المشرفون على الرسالة:

الإسـم: أ.د. يحيى عبد المنعم احمد الدريني **التوقيع:** .....

الوظيفة: أستاذ بقسم الهندسة الميكانيكية – كلية الهندسة – جامعة الإسكندرية – الإسكندرية

الإسـم: د. رولا سمير عفيفي **التوقيع:** .....

الوظيفة: أستاذ مساعد بقسم الهندسة الميكانيكية – كلية الهندسة – الأكاديمية العربية للعلوم والتكنولوجيا والنقل البحري – الإسكندرية

الإسـم: د. ايهم فريد زيدان **التوقيع:** .....

الوظيفة: مدرس بقسم الهندسة الميكانيكية – كلية الهندسة – الأكاديمية العربية للعلوم والتكنولوجيا والنقل البحري – الإسكندرية

الأساتذة المحكمون:

الإسـم: أ.د. علي إسماعيل شحاته **التوقيع:** .....

الوظيفة: أستاذ بقسم الهندسة الميكانيكية – كلية الهندسة – الأكاديمية العربية للعلوم والتكنولوجيا والنقل البحري – الإسكندرية

الإسـم: أ.د. وائل محمد المغلاني **التوقيع:** .....

الوظيفة: أستاذ بقسم الهندسة الميكانيكية – كلية الهندسة – جامعة الإسكندرية – الإسكندرية

الإسـم: أ.د. رولا سمير عفيفي **التوقيع:** .....

الوظيفة: أستاذ مساعد مدرس بقسم الهندسة الميكانيكية – كلية الهندسة – الأكاديمية العربية للعلوم والتكنولوجيا والنقل البحري – الإسكندرية

أودعت هذه الرسالة بالمكتبة بتاريخ / /

إقرار الباحث

أقر بأن المادة العلمية الواردة في هذه الرســـالة قد تم تحديد مصـــدرها العلمي وأن محتوى الرسالة غير مقدم للحصول علي أي درجة علمية أخرى، وأن مضمون هذه الرسالة يعكس أراء الباحث الخاصة وهى ليست بالضرورة الآراء التي تتبناها الجهـة المانحة.

الاسم اسراء ادريس عبدالكريم ادريس

التوقيع .....

التاريخ .....

الأكاديمية العربية للعلوم والتكنولوجيا والنقل البحري

كليـــة الهندســـة والتكنولوجيـــــــا

قسم الهندسة الميكانيكية

عنوان الرسالة

تعزيز كفاءة توربينات الرياح داريوس من خلال التحقيقات التجريبية والعددية لتصميم داريوس المزدوج

إعداد

اسراء ادريس عبد الكريم ادريس

رسالة مقدمة للأكاديمية العربية للعلوم والتكنولوجيا والنقل البحرى لاستكمال متطلبات نيل درجة

ماجستير العلوم

فى

الهندسة الميكانيكية

إشـــراف

أ.د. يحيى الدريني
قسم الهندسة الميكانيكية
كلية الهندسة
جامعة الإسكندرية
الإسكندرية

د. رولا سمير عفيفي
قسم الهندسة الميكانيكية
كلية الهندسة والتكنولوجيا
الأكاديمية العربية للعلوم والتكنولوجيا
والنقل البحري – الإسكندرية

د. ايهم زيدان
قسم الهندسة الميكانيكية
كلية الهندسة والتكنولوجيا
الأكاديمية العربية للعلوم والتكنولوجيا
والنقل البحري – الإسكندرية

2023

الأكاديمية العربية للعلوم والتكنولوجيا والنقل البحري

كليـــة الهندســـة والتكنولوجيـــــــا

قسم الهندسة الميكانيكية

عنوان الرسالة

تعزيز كفاءة توربينات الرياح داريوس من خلال التحقيقات التجريبية والعددية لتصميم داريوس المزدوج

إعداد

اسراء ادريس عبد الكريم ادريس

رسالة مقدمة للأكاديمية العربية للعلوم والتكنولوجيا والنقل البحرى لاستكمال متطلبات نيل درجة

ماجستير العلوم

فى

الهندسة الميكانيكية

إشـــراف

أ.د. يحيى الدريني
قسم الهندسة الميكانيكية
كلية الهندسة
جامعة الإسكندرية
الإسكندرية

د. رولا سمير عفيفي
قسم الهندسة الميكانيكية
كلية الهندسة والتكنولوجيا
الأكاديمية العربية للعلوم والتكنولوجيا
والنقل البحري – الإسكندرية

د. ايهم زيدان
قسم الهندسة الميكانيكية
كلية الهندسة والتكنولوجيا
الأكاديمية العربية للعلوم والتكنولوجيا
والنقل البحري – الإسكندرية

2023